Pre-mRNA splicing repression triggers abiotic stress signaling in plants

Yu Ling[1], Sahar Alshareef[1], Haroon Butt[1], Jorge Lozano-Juste[2], Lixin Li[1], Aya A. Galal[3], Ahmed Moustafa[3], Afaque Ahmad Momin[4], Manal Tashkandi[1], Dale N. Richardson[5], Hiroaki Fujii[6], Stefan Arold[4], Pedro L. Rodriguez[2], Paula Duque[5], and Magdy M. Mahfouz[1, *]

Laboratory for Genome Engineering, Division of Biological Sciences, 4700 King Abdullah University of Science and Technology, Thuwal 23955-6900, Saudi Arabia[1]; Instituto de Biologia Molecular y Celular de Plantas, Consejo Superior de Investigaciones Cientificas-Universidad Politecnica de Valencia, ES-46022 Valencia, Spain[2]; Department of Biology and Biotechnology Graduate Program, American University in Cairo, New Cairo 11835, Egypt[3]; Division of Biological and Environmental Sciences and Engineering, King Abdullah University of Science and Technology, Thuwal, 23955-6900 Saudi Arabia[4]; Instituto Gulbenkian de Ciência, Rua da Quinta Grande 6, 2780-156, Oeiras, Portugal[5]; and Molecular Plant Biology, Department of Biochemistry, University of Turku, FI-20014, Turku, Finland[6]

Corresponding author: [*]Magdy M. Mahfouz (magdy.mahfouz@kaust.edu.sa)

Key Words: Alternative splicing, Pladienolide B, splicing inhibitors, SR proteins, abiotic stress responses, ABA

Running Head: Splicing inhibition triggers abiotic stress signaling

ABSTRACT

Alternative splicing (AS) of precursor RNAs enhances transcriptome plasticity and proteome diversity in response to diverse growth and stress cues. Recent work showed that AS is pervasive across plant species, with more than 60% of intron-containing genes producing different isoforms. Mammalian cell-based assays have discovered various AS inhibitors. Here, we show that the macrolide Pladienolide B (PB) inhibits constitutive splicing and AS in plants. Also, our RNA-seq data revealed that PB mimics abiotic stress signals including salt, drought, and abscisic acid (ABA). PB activates the abiotic stress- and ABA-responsive reporters *RD29A::LUC* and *MAPKKK18::GUS* in *Arabidopsis thaliana* and mimics the effects of ABA on stomatal aperture. Genome-wide analysis of AS by RNA-seq revealed that PB perturbs the splicing machinery and leads to a striking increase in intron retention and a reduction in other forms of AS. Interestingly, PB treatment activates the ABA signaling pathway by inhibiting the splicing of clade A PP2Cs phosphatases while still maintaining to some extent the splicing of ABA-activated SnRK2 kinases. Taken together, our data establish PB as an inhibitor and modulator of splicing and a mimic of abiotic stress signals in plants. Thus, PB reveals the molecular underpinnings of the interplay between stress responses, ABA signaling, and post-transcriptional regulation in plants.

Introduction

Plants employ intricate molecular mechanisms to respond to growth, developmental, and environmental cues (Zhu, 2002; Shinozaki and Yamaguchi-Shinozaki, 2007). The ability of plants to adapt to these ever-changing cues mainly results from the molecular plasticity of their genomes and epigenomes (Chinnusamy et al., 2008; Springer et al., 2016). For example, gene regulation plays a major role in coordinating plant responses to growth, developmental, and stress cues. The plasticity of the transcriptome and the diversity of the proteome are essential for helping plants adapt and cope with environmental stresses (Pikaard and Mittelsten Scheid, 2014). Gene expression involves several regulatory layers, including transcription and pre-mRNA processing through capping, splicing, and polyadenylation, as well as mRNA surveillance and export. The splicing machinery is regulated at the levels of transcription and pre-mRNA splicing under environmental stress conditions (Filichkin et al., 2014).

In photosynthetic eukaryotes, the vast majority of genes (>90%) contain introns (Szarzynska et al., 2009; Labadorf et al., 2010). To generate the mature mRNA, these introns must be precisely excised and the exons joined together. This splicing of precursor mRNAs (pre-mRNAs) is mediated by the spliceosome, a highly dynamic, megadalton-sized, complex machinery composed of small nuclear ribonucleoproteins (snRNPs) and many (>200) associated proteins. Also, splicing is regulated by a variety of upstream effectors that feed stress and growth signaling information to the transcriptional and post-transcriptional regulatory machinery (Jurica and Moore, 2003; Will and Luhrmann, 2011; Filichkin et al., 2015). The assembly of the spliceosome on the pre-mRNA requires conserved sequences that determine the exon/intron boundaries, including a 5' splice GU, a 3' splice site AG, and a branch-point (BP) with a conserved A residue close to the 3' SS (Will and Luhrmann, 2011). Spliceosome assembly requires dynamic RNA–RNA, RNA–protein, and protein–protein interactions, which are mediated by splicing machinery proteins and many associated and regulatory proteins, including the serine/arginine rich (SR) protein and heterogeneous nuclear RNP (hnRNP) families (Filichkin et al., 2015).

Alternative splicing (AS) involves the production of multiple mRNA isoforms from a single gene. AS expands and increases proteome diversity and the number and levels of mRNA isoforms. Therefore, AS constitutes an important regulatory step in post-transcriptional gene expression. AS is regulated in a cell type-, tissue-, and developmental stage-specific manner as well as by stress and growth cues. AS is predominant in humans, where more than 95% of intron-containing genes are alternatively spliced. The frequency of AS events in plants ranges from 40 to 61%, which is lower than that of mammalian systems but much higher than originally expected (Filichkin et al., 2010; Marquez et al., 2012). The estimate of AS in plants is likely to increase when mRNAs from different tissues, developmental stages, and stress conditions are analyzed. Different modes of AS include exon skipping, alternative 5' or 3' SS selection and intron retention. In mammals, exon skipping is the predominant mode of AS, whereas in plants, intron retention is predominant. Thus, AS in mammals enriches the diversity of the proteome and AS of some genes can be attributed to different disease states. By contrast, in plants, exon skipping occurs in a small fraction of AS genes. The majority of AS events in plants generate isoforms with intron retention and a premature termination codon (PTC) (Reddy et al., 2013; Staiger and Brown, 2013). The production of non-functional isoforms could be used to control the levels of functional isoforms and could thus play a regulatory role. PTC isoforms are degraded through the nonsense-mediated decay pathway (Filichkin et al., 2015).

Several reports have implicated AS in the regulation of plant responses to environmental stresses (Staiger and Brown, 2013; Filichkin et al., 2014). AS modulates the expression of stress-induced genes, and splicing factors regulate splice site selection in response to environmental stimuli (Palusa et al., 2007; Duque, 2011; Ding et al., 2014; Feng et al., 2015). SR proteins play major roles in constitutive splicing (CS) and AS by facilitating exon identity, functioning as molecular adaptors linking the pre-mRNA to the splicing machinery, and affecting all forms of RNA metabolism including expression, processing, transport, and translation or decay (Howard and Sanford, 2015). Environmental and hormonal stimuli modulate the AS patterns of SR proteins in *Arabidopsis thaliana* (Tanabe et al., 2007). Under high salinity conditions, the pre-mRNA of SR proteins undergoes AS due to the use of alternative 5' and 3' splice sites, resulting in intron retention isoforms and the formation of a PTC (Cruz et al., 2014; Ding et al., 2014).

Abscisic acid (ABA), a plant stress hormone, plays major roles in abiotic stress adaptation. ABA binds to the PYR/PYL/RCAR family of receptors, which form ternary complexes with clade A protein phosphatases type 2C (PP2Cs), thereby abrogating their inhibitory effects on SNF1-related protein kinases 2 (SnRK2.2/3/6) and leading to the activation of the ABA signaling pathway (Fujii and Zhu, 2009; Fujita et al., 2009; Ma et al., 2009; Park et al., 2009; Santiago et al., 2009; Umezawa et al., 2009; Vlad et al., 2009). Interestingly, mutations in various splicing factors affect plant stress and/or hormonal sensitivity. For example, *sad1* mutant plants are hypersensitive to ABA; the *sad1* mutation leads to errors in splice site selection, thereby increasing the frequency of AS events. These effects are particularly prominent under salt stress. The *sad1* mutant is defective in the dynamic regulation of splicing. Moreover, *SAD1* overexpression (*SAD1-OE*) leads to increased splicing precision and efficiency and improves plant tolerance to abiotic stress (Cui et al., 2014). Moreover, nuclear cap binding complex subunit proteins (CBP20/80) may facilitate the co-transcriptional assembly of the spliceosome (Laubinger et al., 2008). Therefore, co-transcriptional splicing of select genes whose splicing occurs co-transcriptionally may be affected. CBP20 and CBP80 modulate the salt-stress response, implicating these proteins in the interplay between splicing and stress responses (Kong et al., 2014). Furthermore, the SR-like protein SR45 interacts with the spliceosomal proteins U1-70K and U2AF35b, indicating that it plays a role in facilitating spliceosomal assembly or rearrangement (Day et al., 2012). The *sr45-1* mutant is hypersensitive to ABA treatment, implying that SR45 functions in the interplay between ABA signaling, splicing, and stress responses (Carvalho et al., 2010). Another example is the spliceosomal factor SNKW/Ski-interacting protein (SKIP), which interacts with SR45 to regulate AS in abiotic stress responses (Lim et al., 2010; Wang et al., 2012).

Recent advances in RNA-sequencing technologies have revolutionized AS studies in diverse eukaryotic species, including plants (Reddy et al., 2013; Staiger and Brown, 2013; Conesa et al., 2016). However, methods are needed to probe the function of a single or multiple proteins in a noninvasive, tunable, reversible manner to uncover the molecular underpinnings of AS regulation in plants at different developmental stages or in response to stress and growth cues. Employing AS inhibitors may help reveal the hierarchical control and coordination of the response of AS to different developmental and stress cues, thereby opening up the possibility of engineering plants to adapt to or tolerate abiotic stresses. Chemical-genetic screens aim at

identifying synthetic or natural chemical compounds that affect a specific response and at uncovering their molecular targets (McCourt and Desveaux, 2010). These compounds can be used as tools to dissect molecular biological functions and as agents to treat diseases. For example, Trichostatin A inhibits class I and II mammalian histone deacetylases and trapoxin also inhibits histone deacetylases. These two inhibitors have been used to elucidate the roles of histone acetylation and chromatin structure and function in an epigenetic context (Gray and Dangond, 2006). On the other hand, pyrabactin, a synthetic ABA agonist, was used to identify ABA receptors and signaling mechanisms in plants (Park et al., 2009). Pladienolide B (PB) is a naturally occurring macrolide with antitumor activity that was isolated from *Streptomyces platensis*. The potential molecular target of PB was identified as the SAP130 protein of the splicing factor SF3b complex (Kotake et al., 2007). The use of a fluorescently tagged PB probe confirmed the subnuclear localization of the drug in enriched snRNP nuclear speckles. PB treatment of mammalian cells leads to the accumulation of unprocessed mRNA, which is consistent with the direct inhibition of spliceosome assembly and/or stability and impaired U2 snRNP function (Rymond, 2007). Binding of PB derivatives to the SF3b complex of the spliceosome leads to growth inhibition in cancer cells. Therefore, in mammalian cells, PB is a potent antitumor agent, and its synthetic derivatives are currently being tested in clinical trials as anticancer agents. Similarly, spliceostatin A binds to the SF3b complex and inhibits splicing (Kaida et al., 2007).

In the current study, we investigated whether splicing inhibitors in mammalian cells would exhibit the same inhibitory effects in plant cells and could be used to probe the molecular functions of the splicing machinery. Subsequently, we used these splicing inhibitors to tease apart the interplay between splicing inhibition and AS regulation in response to abiotic stress conditions. Our screening identified PB as a potent inhibitor of plant growth and development and revealed that it exhibits selective and potent inhibitory effects on splicing in plants. Ultra-high coverage RNA-sequencing (RNA-seq) and analysis revealed that PB treatment causes ABA and stress-like effects and leads to differential gene expression reminiscent of ABA and abiotic stress treatments. Moreover, our analysis of the effects of PB on AS revealed that PB causes significant intron retention and the formation of splice variants related to abiotic stress. Our *in vivo* data from plants treated with PB show that it mimics stress signals, in a manner reminiscent of ABA, osmotic, and drought treatments, corroborating the RNA-seq data. Furthermore, PB

exhibited drought- and ABA-like effects, including significant activation of the *RD29A* and *MAPKKK18* stress promoters, closure of stomata, and hypersensitivity of the *sr45-1* mutant. Therefore, our data establish PB as an effective inhibitor of splicing in plants that can be used to elucidate the molecular underpinnings of the interplay between abiotic stress signals, ABA signaling, and the regulation of splicing.

RESULTS

PB inhibits Arabidopsis growth and development

Several studies have shown that small molecules, bacterial fermentation products, and their synthetic derivatives can target spliceosomal proteins and modulate *in vivo* splicing and AS in mammalian cells (Bonnal et al., 2012). The effects of these molecules on plant growth and development and their molecular functions have not yet been investigated. Therefore, we tested these compounds in a targeted chemical genetic screen to examine their effects on the growth and development of Arabidopsis and to investigate whether they affect the proteins of the spliceosomal machinery. We used several indole derivatives (including indole, 3-(2-bromomethyl) indole, 6-methylindole, 2,5-dimethylindole, indole-3-carboxylic acid, 5-bromoindole-2-carboxylic acid, and 7-bromo-6-azaindole) that were shown to selectively bind to SR proteins and to inhibit exon splicing of enhancer-dependent introns (Soret et al., 2005; Bonnal et al., 2012). Moreover, we used the bacterial fermentation product PB, which was previously shown to interact with the SF3b1 complex and modulate AS, TG003, a benzothiazole inhibitor of the SR protein kinase CLK1, and the splicing inhibitor isoginkgetin (Kotake et al., 2007; O'Brien et al., 2008; Nishida et al., 2011). To test the effects of these compounds on primary root growth in Arabidopsis, we transferred Arabidopsis (Col-0) seedlings grown on MS medium for 5 days post germination (dpg) to control MS medium or to MS medium supplemented with different concentrations of indole and its derivatives, or a much lower concentration of PB. The transferred seedlings were allowed to grow for an additional 4 days post-transfer (dpt). We examined two regions of the root, region A, which grew before transfer, and region B, which grew after transfer; this allowed us to study the effects of the drug on primary root (PR) growth (Duan et al., 2013). Interestingly, PR growth was sensitive to some of

the indole derivatives and very sensitive to PB, indicating that these compounds may interfere with fundamental processes in plant growth and development (Figure 1).

To further investigate and determine the effects of PB on PRs, we grew Arabidopsis seedlings for 5 days (5 dpg) and transferred them to control MS medium or MS medium supplemented with different concentrations of PB (0.1, 0.2, 0.5, and 1μM) (Supplementary Figure 1). Our results show that PR growth is sensitive to different concentrations of PB. Since PB and spliceostatin A (SSA) both affect AS in mammalian cells (Kaida et al., 2007; Kotake et al., 2007), we tested whether PB and SSA have the same effects. Surprisingly, we found that PR growth under SSA treatment was only very slightly reduced compared to that on control medium, indicating that SSA does not strongly inhibit PR growth (Supplementary Figure 1). Next, we investigated the effects of PB on plant growth and development by examining its effects on Arabidopsis seed germination. Mature Arabidopsis seeds are composed of the testa, a dead protective outer layer, covering a single layer of endosperm cells encompassing the embryo. Arabidopsis seed germination begins with rupture of the testa, followed by simultaneous rupture of the endosperm and protrusion of the radicle. Under optimal conditions, these steps can be completed within 36 h (Piskurewicz et al., 2008). Therefore, we tested the effects of different concentrations of PB on the progression of germination via these steps. Our data reveal that PB treatments led to delayed germination compared to control treatments (Figure 1).

PB perturbs splicing and causes intron retention in a select group of genes

Since previous studies in mammalian cells demonstrated that PB can affect splicing, we set out to test whether PB affects CS and/or AS in plants. Therefore, we selected a group of alternatively spliced genes (Pandey et al., 2002; Leviatan et al., 2013; Jang et al., 2014), including the microsomal ascorbate peroxidase gene *APX3* (AT4G35800), the histone acetyl transferase gene *HAC04* (AT1G55970), *Arabidopsis thaliana SENESCENCE1* (*ATSEN1*; AT4G35770), and the NADP-Malic enzyme gene *NADP-ME2* (AT5G11670). We treated one-week-old Col-0 Arabidopsis seedlings with 0.5, 1.0, and 5.0 μM PB for 6 or 24 h and used primers flanking selected introns in RT-PCR analysis to determine the levels of processed and unprocessed mRNA isoforms. Our data reveal that PB caused intron retention and accumulation of aberrantly processed pre-mRNA, interestingly, the intron retention intensity at 6h treatment was higher than

that at 24h treatment, a plausible interpretation of these data could be that the plants adapt to the chemical stress after longer incubations with the PB splicing inhibitor (Figure 2). Furthermore, our data show that the seedlings treated with 5 μM PB recover after transferring to control media lacking PB indicating that the PB effects are reversible (Supplementary Figure 2). In conclusion, our data show that PB severely perturbs the splicing process, generating splicing stress, and that the PB effects are reversible.

PB treatments produce gene expression patterns similar to abiotic stress treatments

Our data showing that PB inhibits splicing of a set of genes in Arabidopsis prompted us to investigate the genome-wide effects of PB on this process. To this end, we performed RNA-seq using the Illumina-HiSeq platform (Illumina Inc. San Diego, CA, USA) on one-week-old Col-0 Arabidopsis seedlings treated with 5 μM PB for 6 and 24 h. We sequenced eight libraries, including four libraries from 6 and 24 h DMSO-treated plants (controls) and four libraries from 6 and 24 h PB-treated plants. Our RNA-seq generated more than 150 million reads per library, approximately 90% of which could be mapped to the TAIR10 reference genome (Version TAIR10). Mapping of reads to gene models of the TAIR10 reference genome revealed that approximately 88–90% mapped to exons, 4–6% mapped to introns, and 6–7% mapped to intergenic regions (Supplementary Figure 3). Moreover, our data indicate that as more reads were generated, the number of newly discovered genes plateaued, indicating that our sequencing reached saturation and had extensive coverage (Supplementary Figure 3).

Next, we asked whether the PB treatments would have genome-wide effects on gene expression. Therefore, we performed clustering analysis of transcript levels between the 6/24 h treatments and the controls, finding that 806 genes were differentially expressed after 6 h of PB treatment and 893 genes were differentially expressed after 24 h of treatment. Furthermore, 496 genes showed consistent up- or downregulation after 6/24 h treatments (Supplementary Figure 4). The differentially expressed genes (DEGs) after 6 and 24 h of PB treatment versus the control overlapped with those identified as responsive to ABA and abiotic (drought and salt) stress, as indicated in the GENEVESTIGATOR databases, suggesting that PB treatments trigger a transcriptional stress response in the plant cell (Figure 3, Supplementary Figure 4). Furthermore, we performed functional annotation of the DEGs using DAVID software (Huang da et al.,

2009b). Our functional analysis revealed that PB treatments trigger responses that are enriched in the abiotic stresses and hormonal responses categories (Figure 3). Intriguingly, differentially expressed genes in 6/24 h treatments were mapped onto the abscisic acid activated signaling network (Supplementary Figure 4).

PB treatment results in significant global intron retention and reduces other forms of AS

To investigate the effects of PB on AS, we used a recently developed pipeline to identify AS events in Arabidopsis (Cui et al., 2014). Using this pipeline, we generated high-confidence splice junction datasets for the eight libraries. These datasets were compared to the annotated genes and used to identify all AS events, including alternative 5' splice sites, alternative 3' splice sites, coordinate cassette exons, cassette exons, and intron retention. We compared the differences in AS patterns between the PB treatments and control samples. Surprisingly, we found that PB treatment significantly reduced all forms of AS, except intron retention, compared to the control. As indicated in Figure 4, PB treatment decreased the number of alternative 5'splice site events from 310 in the controls to only 35 in the PB treatment groups. Similarly, PB treatment decreased the number of alternative 3' splice site events from 400 in the controls to only 48 in the PB treatment group. Also, the number of cassette exons was reduced from 145 in the control to 23 in the PB-treated groups and the number of coordinate cassette exons was reduced from 17 in the control to only 2 in the PB-treated groups.

To investigate the effects of PB on intron retention, we plotted the expression intensity of introns and exons between the PB-treated and untreated samples. As indicated in Figure 4, PB treatments for 6 and 24 h resulted in significant global and widespread intron retention. Next, we selected six different genes that showed intron retention in the 6 and 24 h datasets, respectively, for visualization using the Integrated Genomics Viewer (IGV, see Supplementary Figure 5). Furthermore, we compared the counts of exonic and intronic reads using Fisher's Exact Test. We identified 21,151 introns from 8268 genes that were significantly retained at 6 h treatment and 11,867 introns from 5483 genes that were significantly retained at 24 h treatment, indicating that the splicing patterns of about 37% and 25% of intron-containing genes were significantly inhibited at 6 h and 24 h treatments, respectively. Furthermore, 10,704 introns were significantly retained in 5202 genes at 6 and 24 h treatments. Our data demonstrate the widespread and global

increase in intron sequences in PB-treated samples at 6 and 24 h (Figure 4, Supplementary Figure 6). Such an increase was not observed for exons, indicating the widespread retention of introns in PB-treated samples. In an effort to assess if PB affects pre-mRNA splicing in general, i.e. constitutive splicing in addition to alternative splicing, we compared our datasets of retained introns in the 6 and 24h PB treatments against a high-confidence list of 110,254 CS introns derived from Mao et al 2014 (Mao et al., 2014). We observed that 93% (19,649) and 92% (10,885) of the retained introns in the 6 and 24h PB treatments overlapped with CS introns, respectively. This high overlap suggests that PB perturbs the splicing reaction in general and consequently, reduces all cases of alternative splicing. Further sequence analysis of intron-retained transcripts revealed that most of them were predicted to generate premature stop codons and truncated proteins if translated (Supplementary Figure 7). Therefore, PB can significantly affect the ratio between functional and non-functional transcripts, thereby affecting plant responses to splicing stress.

PB treatment results in aberrant splicing in stress-responsive and stress-related genes

Next, we examined the functional categories of the genes with perturbed splicing in response to PB treatment. We identified more than 8000 genes with perturbed splicing after 6 h PB treatment and found that the majority of these genes show intron retention. We employed DAVID software to determine the functional categories of genes with perturbed splicing (Huang da et al., 2009b, a), and we found that these genes were enriched in functional categories including response to abiotic stress, protein localization and transport, metabolic processes, and RNA processing (Figure 5, Supplementary Figure 6). These findings suggest that PB perturbs the splicing machinery or splicing factors that control stress responses. Alternatively, inhibiting the splicing machinery could trigger a stress response. Further analysis using GENEVESTIGATOR revealed that most of the genes perturbed in splicing belong to the category abiotic stress responses (Zimmermann et al., 2004). For instance, we found that some stress-related genes showed aberrant splicing, including *ABI1*, *ABH1*, *ABF3*, *AREB3*, and *SAD1*. Subsequently, we used RT-PCR analysis to validate the intron retention events of these ABA- and stress-related genes and found that the RT-PCR data agreed with the RNA-seq data (Figure 6).

Differential gene expression and differential AS are regulated in response to PB treatment

We then investigated whether the set of genes that are differentially expressed in response to PB treatment are also differentially spliced. Analysis of our RNA-seq data showed that 806/893 genes were differentially expressed after 6/24 h of treatment. Among the DEGs, 643 were upregulated and 163 were downregulated after 6 h of treatment, while 711 genes were upregulated and 182 were downregulated after 24 h of treatment. Functional categorization revealed that these DEGs are involved in ABA and abiotic stress responses. However, when we compared the DEGs with genes exhibiting differential AS, specifically IR, we found that a large fraction of these genes overlapped (27%), indicating that these two processes are co-regulated. Functional categorization of overlapping genes, which were both differentially expressed and exhibited differential AS in response to PB treatment, revealed that this group of genes is closely related to the response to abiotic stress (Supplementary Figure 8). However, it remains to be determined whether these overlapping genes play a major role in coordinating the PB response at the transcriptional and post-transcriptional levels. In the 6 h treatment group, the predominant functional categories that represent the DEGs include response to chitin, response to organic substance, and response to carbohydrate stimulus, whereas in the 24 h treatment group, the predominant functional categories include response to temperature stimulus, response to oxidative stress, and response to heat. Moreover, the predominant functional categories that represent the differential AS genes include responses to different abiotic stresses. Overall, these data indicate that PB treatment is perceived as a stress signal in plants and is regulated at the transcriptional and post-transcriptional levels.

PB activates abiotic stress- and ABA-inducible genes

Because gene expression analysis and functional annotation of DEGs revealed that PB triggers abiotic stress and hormonal responses, we investigated whether PB mimics stress and hormonal signals using Arabidopsis plants expressing the firefly luciferase (*LUC*) reporter gene under the control of a stress-responsive promoter. *RD29A*, a well-studied stress-responsive promoter, contains ABA responsive elements (ABREs) and dehydration response elements (DREs) (Yamaguchi-Shinozaki and Shinozaki, 1994). This promoter responds to salt, osmotic, and cold stress, as well as ABA treatment (Ishitani et al., 1997; Mahfouz et al., 2012). Therefore, this promoter contains several stress and hormonal elements that were shown to be induced by PB in our gene expression analysis. Subsequently, we determined whether PB would mimic a stress

signal and activate the *RD29A* promoter. For this, we used an Arabidopsis C24 line stably overexpressing *LUC* driven by the *RD29A* promoter (*RD29A::LUC*). Treatment of C24 *RD29A::LUC* plants with different concentrations of PB led to significant activation of the *RD29A* promoter, as evidenced by LUC signals. Specifically, 0.5 μM PB led to activation of *RD29A::LUC*, and 5 μM PB led to significant activation compared to treatment with 100 μM ABA (Figure 7 and Supplementary Figure 9). These results indicate that PB mimics a stress signal that significantly activates the stress-responsive *RD29A* promoter. Because the *RD29A* promoter contains both ABREs and DREs, and the DREs can be activated by osmotic and cold stress independently of ABA, the PB-induced activation of *RD29A* could be ABA-dependent or ABA-independent. Therefore, we tested the effect of PB on the activation of the ABA-responsive promoter *MAPKKK18* (Okamoto et al., 2013). Our GUS staining experiment revealed that the *MAPKKK18* promoter was induced by PB (Supplementary Figure 10). To confirm the LUC bioluminescence and GUS staining data, we performed quantitative RT-PCR on Arabidopsis seedlings treated with PB. Our data show a strong induction of *RD29A*, *RD29B* and *MAPKKK18* genes in PB treated samples compared to the controls (Supplementary Figure 10). Therefore, these data corroborate our reporter assays data, and imply that PB affects the regulatory system that plays a role in abiotic stress and ABA responses.

PB mimics ABA signaling and modulates stomatal aperture

ABA is a phytohormone that regulates plant growth and adaptation to stress, with a key role in the control of stomatal aperture. Guard cells are capable of autonomously synthesizing ABA, which induces stomatal closure under low-humidity conditions (Bauer et al., 2013). Because our data on differential gene expression patterns and the induction of stress promoters by PB suggested PB triggers ABA response in plants, we further explored the effects of PB on regulation of stomatal aperture. We therefore incubated epidermal peels of wild-type Arabidopsis and fava bean (*Vicia faba*) leaves in opening solution under elevated light conditions to promote stomatal opening. Applying exogenous ABA led to stomatal closure. Similarly, PB treatment led to stomatal closure at a level comparable to that of ABA treatment, which helps confirm the finding that PB can activate the ABA signaling pathway (Figure 7).

The effects of PB on differential AS of splicing factors

Because our data revealed that the macrolide PB is implicated in the inhibition of splicing and AS in plant cells, we attempted to investigate the effects of PB treatment on the splicing of genes encoding components of the splicing machinery and regulatory genes. For example, SR proteins are implicated in the execution and regulation of splicing reactions and are responsive to abiotic stresses and ABA (Barta et al., 2010; Duque, 2011; Reddy and Shad Ali, 2011). We examined Arabidopsis SR genes using the IGV junction browser, which revealed significant intron retention in these genes response to PB treatment specifically at 6 h (Supplementary Figure 11). We validated the RNA-seq data via RT-PCR analysis using exonic primers flanking the intronic sequences, which confirmed that SR genes respond to PB treatment by accumulating higher levels of unprocessed mRNA as evidenced by higher levels of intron retention (Supplementary Figure 11). Moreover, our data show that most of the SR genes retain significant levels of functional isoforms even at 6 h treatment, where intron retention levels are the highest. These data support the molecular role of SR proteins as essential players in splicing and different steps of RNA metabolism and regulation. Additionally, less nonfunctional levels of isoforms were accumulated at 24 h indicating that plants adapt to the PB effects and increase the repertoire of functional transcripts of essential and key genes.

PB regulates the localization of the splicing factor SR45, and the *sr45-1* mutant is highly sensitive to PB treatment

SR45 interacts with the U1 snRNP 70K protein, as revealed by yeast two-hybrid analysis (Golovkin and Reddy, 1999). SR45 is structurally distinct from SR proteins and has two RS domains flanking the RRM domain. One of the most important sub-nuclear bodies is the nuclear speckle, which localizes to the inter-chromatin space and serves as a storage compartment for a variety of splicing and processing factors (Reddy et al., 2012). Therefore, nuclear speckles supply the needed splicing and processing factors for active transcription processes, to produce mature mRNAs ready for export. SR proteins are concentrated in nuclear speckles, with diffuse distribution in the nucleoplasm and Cajal bodies (Tillemans et al., 2006). Various experiments have indicated that SR proteins localize to the nucleus and target to nuclear speckles. Notably, the size and shape of nuclear speckles are determined by developmental, stress, metabolic state, transcriptional activity, and hormonal factors. SR protein localization and dynamics are affected by environmental stress (Duque, 2011). Since PB is a splicing inhibitor that mimics stress signals

and has a dramatic effect on gene expression profiles, and it regulates gene expression patterns in a similar manner to that of abiotic stress and ABA treatments, we investigated whether PB affects the sub-nuclear localization and distribution of SR45. SR45 mainly localizes to nuclear speckles. Abiotic stress treatments including heat and cold result in the formation of large and irregularly shaped speckles (Ali et al., 2003). We therefore treated the *AT-GFP-SR45OE* lines with 5 μM PB, which resulted in the redistribution and re-localization of GFP-SR45 to nuclear speckles, suggesting that PB plays an important role in the regulation of splicing (Figure 8).The *sr45-1* loss-of-function mutant exhibits delayed flowering, with abnormal floral organs and reduced root growth (Ali et al., 2007). Interestingly, the SR genes in this mutant exhibit altered AS patterns, which might be the reason for these phenotypes. *SR45* produces two isoforms: *SR45.1* can complement the delayed flowering and flower defects phenotype, and *SR45.2* can complement the reduced root growth phenotype (Zhang and Mount, 2009). The *sr45-1* mutant also exhibits altered responses to ABA and glucose treatment. SR45 functions as a negative regulator of ABA signaling (Carvalho et al., 2010). Since SR45 is a negative regulator of ABA signaling and displays different splice variants in response to PB treatment, we investigated the response of the *sr45-1* mutant to PB. Our data showed that the *sr45-1* mutant was overly sensitive to PB treatment, indicating that the global PB inhibitory effect on splicing and stress responses is enhanced by the lack of SR45 function. Moreover, our RT-PCR data showed that the splicing patterns of the SR34a and HAI1 genes are different in *sr45-1* and Col-0 under PB treatments (Supplementary Figure 12). This could explain why the *sr45-1* mutant is hypersensitive to PB. *sr45-1* is hypersensitive to PB because two inhibitory effects on splicing accumulate, one due to global PB-mediated inhibition and the second due to lack of SR45 function.

PB regulates differently the splicing of PP2C phosphatases and ABA-activated SnRK2 kinases

Our data reveal that PB activates ABA signaling. Such activation might result from the direct binding of PB to ABA receptors and subsequent inhibition of PP2C phosphatases, thereby relieving their inhibitory effect on ABA-activated SnRK2 kinases and leading to the activation of ABA signaling. Alternatively, PB could selectively and differentially regulate the splicing of the PP2C phosphatases and SnRK2 kinases. To investigate whether PB could bind to PYR/PYL receptors, we performed computational docking simulations of PB to PYR/PYL receptor

structures. Our molecular docking studies predict sub-micromolar binding affinity among some PYR/PYLs and PB in the open receptor confirmation but not in the closed receptor conformation. These results suggest that PB, but not Spliceostatin A, has putatively similar binding strengths with PYR/PYL compared to ABA (Supplementary Table 1, Supplementary Figure 13, and supplementary methods). However, in contrast to ABA, PB does not fit into the closed receptor conformation, which precludes the allosteric change induced by ABA in the closed receptor conformation to inhibit PP2Cs. Therefore, we tested whether such binding occurs *in vivo* using yeast two-hybrid analysis. Our data reveal that PB is incapable of mediating an interaction between the PYR/PYL receptors and PP2Cs (Supplementary Figure 14).

To investigate the second possibility, we tested whether PB inhibits regulators of ABA signaling by performing RT-PCR on all PP2Cs and SnRK2s. Interestingly, we found that the negative ABA regulators PP2Cs accumulated significant levels of nonfunctional isoforms, with the absence of functional isoforms sufficient to inhibit the ABA signaling pathway. By contrast, although SnRK2.2 and 2.3 accumulated nonfunctional isoforms, a significant fraction of functional isoforms remained. Furthermore, *SnRK2.6* did not accumulate nonfunctional isoforms and substantial functional isoforms remained (Supplementary Figure 15). Recently, the splice variant *HAB1.2* was shown to function as a positive regulator of the ABA pathway (Wang et al., 2015; Zhan et al., 2015). Therefore, we investigated the effects of PB treatment on the formation of this PP2C isoform. Interestingly, our data reveal the accumulation of the *HAB1.2* splice variant, which functions as a positive regulator of the ABA pathway (Supplementary Figure 16). These data substantiate the selective modulation of negative regulators of the ABA pathway via splicing regulation.

ABA insensitive mutants are less sensitive to PB treatments

To investigate to what extent PB effects are mediated by ABA signaling, we tested PB sensitivity in several mutant impaired in ABA signaling. Interestingly, our data reveal that the *abi1-1C* mutant (Umezawa et al., 2009) exhibited partial resistance to PB treatments. We performed different assays including ABA-mediated inhibition of seed germination, seedling establishment and root growth. In the seedling establishment assay nearly 80% of *abi1-1C* seedlings produced true leaves compared to less than 20% of Col-0 seedlings, after 7 days on MS media

supplemented with 1μM PB (Figure 9). Similarly, the *abi1-1C* mutant exhibited 90% germination compared to less than 60% of Col-0 wt seeds on MS media supplemented with 1μM PB (Figure 9). Moreover, the triple *snrk2.2/3/6* mutant (Fujii and Zhu, 2009) also exhibited higher germination rate on MS media supplemented with PB 1μM PB, when compared to the Col-0 wt plants (Figure 9). Furthermore, roots of *snrk2.2/3/6* and 35S:HAB1 (Saez et al., 2004) 35S:HAB1 overexpresses HAB1 ORF, so no splicing required) seedlings grown on 1μM PB showed reduced inhibition of root growth than those of the Col-0 wt seedlings (Figure 9). These data indicate that PB effects are mediated, at least in part, through ABA signaling, thereby linking the splicing stress generated by PB and abiotic stress responses.

DISCUSSION

Environmental stresses modulate plant AS responses (Filichkin et al., 2014). Little is known about the interplay between the splicing machinery, post-transcriptional regulation of gene expression, and stress responses. Several mutants of splicing machinery components or regulatory proteins have been identified and were found to be highly sensitive to environmental stresses and ABA. RNA-seq analyses have revealed that AS plays an important role in plant responses to various stress or growth conditions. Because plant cells lack an *in vivo*-splicing system, there is a pressing need to identify chemical compounds capable of manipulating the splicing machinery. Such compounds would have clear advantages in studies of AS, including the ability to be used in a dose-dependent manner, tunability, reversibility, and conditionality. In this study, we identified PB as a splicing inhibitor that could potentially be used to probe the splicing machinery in plants under a variety of cellular conditions and developmental stages.

PB exhibited significant inhibitory effects on plant growth and development in a concentration-dependent manner. For example, PR growth in various Arabidopsis ecotypes was significantly inhibited under 0.5μM PB treatment (Supplementary Figure 17). To determine whether the effects of PB are species-specific, we examined the effects of PB on different plant species, including tomato and rice, and found that PB treatments indeed led to significant inhibition of PR growth and affected overall plant growth and development (Supplementary Figure 17). Since the main function of PB in mammalian cells involves splicing inhibition, we investigated the effects of PB on splicing of a subset of genes that have been shown to be alternatively spliced. Our data

reveal that PB selectively modulates CS, AS, and a combination of both in plants. PB binds to the SF3B1 complex in mammalian cells, thereby inhibiting splicing. Therefore, the effects of PB on plants could be mediated by the targeted inhibition of the splicing machinery or the SF3B1 complex. We did not obtain any viable mutant in Arabidopsis for the genes corresponding to orthologs of the SAP130, SAP145, and SAP155 proteins, which bind to PB in mammalian cells. Application of CRISPR/Cas9-based genome engineering should facilitate the generation of protein variants that are functional but incapable of binding to PB (Mahfouz et al., 2014). Such variants would be crucial for developing tools for targeted manipulation of the splicing machinery and revealing the cellular effects of PB.

To investigate the effects of PB on CS and/or AS in plants, we performed genome-wide analysis of the effects of PB on gene expression patterns and on CS and AS. We observed that the splicing patterns of about 37% and 25% of intron-containing genes were significantly perturbed at 6 h and 24 h treatments, respectively. However, we can not exclude the possibility that the number of affected genes with splicing perturbations could be higher. This potential underestimation can be attributed to the inability to assess differences in splicing of lowly expressed genes, which have an insufficient number of reads for statistical testing. Therefore, the estimates of the number of intron-containing genes with aberrant splicing in the 6h and 24h PB treatments should be considered conservative. Notably, we found that the majority of retained introns (>92%) in our 6 and 24h PB treated datasets corresponded to a high-confidence dataset of constitutively spliced introns obtained by (Mao et al., 2014). Thus, it appears that PB acts predominantly to inhibit components of the basic splicing machinery, such that splice sites are no longer reliably recognized resulting in aberrant levels of intron retention and reduced levels of alternative splicing. Therefore, PB treatments would lead to general splicing stress. Interestingly, our gene ontology analysis revealed that PB treatment mimics a stress signal and leads to differential expression of genes related to abiotic stress (salt and drought) and ABA. To corroborate the differential gene expression data, we tested the effect of PB on the stress- and ABA-inducible promoters *RD29A* and *MAPKKK18*. PB activated both genes in a dose-dependent manner, indicating that PB mimics stress or ABA signals and activates the ABA pathway. Subsequently, we tested the effects of PB on stomatal aperture, finding that PB application led to stomatal closure, mimicking an ABA signal. Therefore, PB triggers both ABA-mediated transcriptional and stomatal responses.

The *sr45-1* mutant is hypersensitive to ABA treatment. Recently, SR45-associated RNA species (SARs) were identified by RIP-seq. Interestingly, 43 SARs in the ABA signaling network (147 genes) have been identified, indicating that SR45 plays a role in ABA signaling (Xing et al., 2015). Therefore, we tested the effects of PB on the *sr45-1* mutant, finding that this mutant is highly sensitive to PB treatment. Furthermore, PB treatment led to the formation of nuclear speckles in SR45:GFP transgenic lines. These data substantiate the link and the interplay of splicing regulation with PB, abiotic stress, and ABA signals.

SR proteins are splicing regulators that function in various aspects of RNA metabolism, including pre-mRNA splicing. These proteins have diverse and redundant functions in both CS and AS. Post-translational modifications, primarily phosphorylation, determine the biological functions of SR proteins in the nucleus and cytoplasm. The *sr45-1* mutant is hypersensitive to ABA, and our data show that it is also hypersensitive to PB. Interestingly, PB treatment led to the localization of SR45 in nuclear speckles, indicating that this macrolide perturbs splicing. We analyzed the effect of PB on the gene expression profiles of SR proteins, as well as AS of their pre-mRNAs. PB did not affect the expression profiles of these genes. However, PB treatment led to significant intron retention at 6 h treatment. Interestingly, substantial levels of functional isoforms remain under PB treatment indicating the key role SR proteins play in splicing regulation under abiotic stress conditions, thereby implicating SR proteins in the early phase of stress perception and splicing inhibition.

PB treatment activated the ABA signaling pathway, as evidenced by the activation of ABA-responsive promoters including *RD29A* and *MAPKKK18* as well as the global analysis of plant transcriptome after PB treatment. There are two possible explanations for this activation: first, PB functions as an ABA agonist and mediates the binding of PYR/PYL ABA receptors to PP2Cs (negative regulators of ABA signaling), thereby relieving the inhibition of SnRK2 kinases, resulting in the activation of the ABA pathway. Second, negative regulators of ABA signaling, including PP2C, are selectively inhibited at the splicing level, while enough splicing of ABA-activated SnRK2s is maintained, leading to the activation of the ABA signaling pathway. Our *in silico* molecular docking studies suggest, and yeast two hybrid analysis confirms the inability of PB to mediate an interaction among some PYR/PYLs receptors and PP2Cs. These data suggest that PB-mediated activation of ABA signaling does not require activation of ABA receptors.

Therefore, we investigated whether PB leads to differential splicing of negative (PP2Cs) and positive regulators (SnRK2s) of ABA signaling. Unexpectedly, we found a dramatic accumulation of nonfunctional PP2C isoforms, probably sufficient to inhibit the ABA signaling pathway. Therefore, PB triggers ABA signaling via differential splicing of negative and positive regulators respectively.

This work highlights a strong connection between the splicing machinery and ABA signaling. Previous reports have indicated the involvement of RNA metabolism in the regulation of ABA responses, including cap binding protein 20 (CBP20), ABA hypersensitive 1, and SAD1/Lsm5 (Kuhn et al., 2008; Cui et al., 2014). We further extend these findings because we noticed that splicing of PP2C transcripts can be a sensitive step to transduce splicing stress into ABA signaling. Therefore, abiotic stress-induced impairment of RNA splicing is efficiently linked to the generation of ABA responses to attenuate cellular damage. Since PP2Cs are key negative regulators of ABA signaling, the described mechanism might be an adaptive response to efficiently link the stress-induced perturbation of RNA metabolism to a major defensive mechanism to cope with abiotic stress. Indeed induction of RNA chaperons is a major response to different forms of abiotic stress and overexpression of certain splicing factors leads to an increase both in splicing efficiency and stress tolerance (Nakaminami et al., 2006; Cui et al., 2014). Therefore, the availability and levels of splicing factors could affect splicing efficiency under stress conditions. The application of chemical genetics approaches using splicing inhibitors and modulators would reveal key splicing factors that sense and regulate splicing efficiency and accuracy under abiotic stress conditions. Unexpectedly, our work indicates that the ABA signaling pathway is one of the first layers that plant cells use to respond to splicing inhibition or defects. ABA signaling under abiotic stress conditions, as well as enhanced splicing, are used to establish an adaptive response to such conditions.

METHODS

Plant materials and growth conditions

Seeds of wild-type *Arabidopsis thaliana* wild-type Col-0, L*er*, C24 (*RD29A::LUC*), *35S::HAB1, 35S::SR45.1:GFP, MAPKKK18::GUS,* and the *sr45-1, abi1-1C, and snrk2.2/3/6* mutants were

surface-sterilized with 10% bleach for 10 min and stored at 4°C for 2 days (Ali et al., 2003; Carvalho et al., 2010; Bardou et al., 2014). The seeds were plated on Murashige and Skoog (MS) medium agar plates supplemented with 1% sucrose, vitamins and the indicated chemicals. The plates were placed in a growth chamber (Model CU36-L5, Percival Scientific, Perry, IA, USA) under 16 h-white light (~75 μmol m^{-2} s^{-1}) and 8 h-dark conditions at 22°C for germination and seedling growth.

Chemicals

The chemicals 3-(2-bromoethyl) indole (CAS: 3389-21-7), 6-methylindole (CAS: 3420-02-8), 2,5-dimethylindole (CAS: 1196-79-8), indole-3-carboxylic acid (CAS: 771-50-6), 5-bromoindole-2-carboxylic acid (CAS: 7254-19-5), TG003 (CAS: 300801-52-9), 7-bromo-6-azaindole (CAS: 165669-35-2), and indole (CAS: 120-72-9) were purchased from Sigma Aldrich (St. Louis, MO, USA). Isoginkgetin (CAS: 548-19-6) was purchased from Merck KGaA (Darmstadt, Germany). Pladienolide B (CAS: 445493-23-2) was purchased from Bioaustralis (Smithfield, NSW, Australia). Spliceostatin A (CAS: 391611-36-2) was purchased from Adooq Bioscience (Irwin, CA, USA).

RNA extraction and RNA-seq

Total RNA was extracted from seedlings after the indicated treatments (DMSO and different concentrations of PB) for 6 or 24 h using TRIzol Reagent (Catalog No. 15596–026, Invitrogen). Polyadenylated RNA was isolated using an Oligotex mRNA Midi Kit (70042, Qiagen Inc., Valencia, CA, USA). The RNA-seq libraries were constructed using an Illumina Whole Transcriptome Analysis Kit following the standard protocol (Illumina, HiSeq system) and sequenced on the HiSeq platform to generate high-quality paired-end reads.

RNA-sequencing data analysis and gene functional classification

The annotated Arabidopsis gene models were downloaded from TAIR10 (https://www.arabidopsis.org/). TopHat (Version 2.0.10) was used for alignment and to predict splice junctions (Trapnell et al., 2009). Gene expression levels (FPKM value) were calculated using Cufflinks (Version 2.0.0). The DEGs were identified using Cufflink and the limma package in R. Very strict criteria were used to define DEGs: DEGs must simultaneously show

more than 1.8-fold upregulation/downregulation in both replicates, and P-values calculated by limma must be less than 0.05. To filter out false positive junctions, well-studied criteria (i.e., an overhang size of more than 20 bp and at least two reads spanning the junctions) were set as cutoff values (Cui et al., 2014). JuncBASE was used to annotate all AS events based on the input genome coordinates of all annotated exons and all confidently identified splice junctions (Brooks et al., 2011). Fisher's Exact Tests were used to identify differential representation of each type of AS event. For intron retention, Fisher's Exact Tests were performed on the intron-read counts and the corresponding exon-read counts between control and 6 h/24 h drug treatments. The events with p-value < 0.001 were identified as significantly different. In addition, intron retentions uniquely identified in the control or treatment groups were considered significant if there was at least five-fold coverage of support and the p-values of these events were assigned to zero. For alternative 5' SSs and 3' SSs and exon skipping events, Fisher's Exact Tests were performed on the comparisons of the junction-read counts and the corresponding exon-read counts between the control and 6 h/24 h drug treatments. The events with p-values less than 0.05 were identified as significantly different. GO classifications were performed with DAVID software. GO network analysis was performed with EGAN.

RT-PCR and RT-qPCR

For reverse-transcription quantitative PCR (RT-qPCR), DNA digestion of total RNA samples was performed after RNA extraction using an RNase-Free DNase Set (Invitrogen cat. No. 18068-015) following the manufacturer's protocol. The total RNA was reverse transcribed using a SuperScript First-Strand Synthesis System for RT-qPCR (Invitrogen) to generate cDNA. The qPCR was performed as previously described (Wang et al., 2013) using Power SYBR Green PCR Master Mix (Invitrogen) under the following conditions: 95°C for 10 min, then cycles of 95°C for 15 s, 60°C for 1 min. Primers used for RT-PCR are listed in Table S2.

Germination rate assay

Freshly harvested Arabidopsis Col-0 seeds were surface sterilized, plated on control or chemical-containing MS agar plates, placed in a 22°C growth chamber, and photographed at the indicated time points under a stereomicroscope (Nikon, SMZ 25). According to Piskurewicz *et al.*, seeds with radicle emergence were scored as germinated (Piskurewicz et al., 2008).

Root elongation rate assay

Five-day-old seedlings were transferred from ½ × MS medium plates to the indicated chemical-containing MS plates for an additional 3 days unless stated otherwise. The elongated root length after transfer to DMSO plates (control) was set at 1 (100%). The root elongation rates on the chemical-containing plates were calculated as the elongated root length on chemical/elongated root length on DMSO × 100%. Values are means ± SE, n = 20. Significance ($P < 0.05$) was assessed by the Student's *t*-test.

***RD29A::LUC* analysis**

Intact 10-day *RD29A-LUC* plants were treated with 0.05% DMSO, 5 μM PB, or 100 μM ABA for 5–6 h and transferred into 96-well plates (Nunc White polystyrene) containing 100 μl 1 mM D-luciferin (Gold Biotechnology, St. Louis, MO, USA). The plates were incubated for 10 min in the dark before luminescence imaging under a CCD camera (ANDOR) with Solis (version 4.24) software for relative luminous intensity measurements using a TECAN Ultra 96 microplate reader (Aouida et al., 2013).

Stomatal aperture assays

Rosette leaves from 2–3-week-old plants were floated in 50 μM $CaCl_2$ 10 mM KCl 10 mM MES-Tris (pH 6.15) and exposed to light (150 μmol m^{-2} sec^{-1}) for at least 2.5 h. Subsequently, DMSO, PB, or ABA was added to the solution at 20 μM to assay for stomatal closure (Ren et al., 2010). After treatment for 4 h, stomatal apertures in plant tissue in a microscope slide were photographed immediately under a light microscope (Carl Zeiss, Axio Imager.2) at a magnification of 400×. After image acquisition, the width of stomatal apertures was measured with the open access software Image J (Version 1.37) as previously described (Luo et al., 2013). Values are means ± SE, n = 100. Significance ($P < 0.05$) was assessed by the Student's *t*-test.

Subcellular localization of SR45 protein

Five-day-old 35S:SR45.1-GFP transgenic seedlings were incubated in 0.01% DMSO with 5 μM PB for 6 h and viewed under a Zeiss laser-scanning microscope (Carl Zeiss Meta 710, Wetzlar, Germany) with a 488-nm argon laser and a long-pass 530 filter. Serial optic sections were

collected and projected with Zeiss LSM Image Browser software (Carl Zeiss) and Photoshop version 7.0 software (Adobe).

Acknowledgments

We wish to thank members of the Laboratory for Genome Engineering at King Abdullah University of Science and Technology for helpful discussions and comments on the manuscript. We wish to thank Moussa Benhamed for helpful discussions and suggestions and for providing key materials. We wish to thank Sean Cutler for providing Arabidopsis seeds of *MAKPKKK18-GUS*.

Funding

This study was supported by King Abdullah University of Science and Technology. Work in Pedro Rodriguez laboratory was funded by grant BIO2014-52537-R from MINECO. Work in Paula Duque laboratory is funded by grant PTDC/BIA-PLA/1084/2014 from FCT.

Short legends for supporting information

Supplementary Figure 1. Effects of PB and SSA on root elongation rate.
Supplementary Figure 2. Arabidopsis seedlings recovered from PB treatment.
Supplementary Figure 3. High quality of RNA-seq data.
Supplementary Figure 4. Gene expression changed by PB corresponding to stress responses.
Supplementary Figure 5. RNA-seq data demonstrates PB inducing intron retention in a group of genes.
Supplementary Figure 6. Genes with intron retention in PB treatments are associated with stress responses.
Supplementary Figure 7. Comparison of proteins Encoded by known transcripts (top) and those by novel transcripts (Bottom).
Supplementary Figure 8. Functional categorization of overlapping DE and IR genes.
Supplementary Figure 9. Low concentration of PB induced RD29A-LUC activation in Arabidopsis seedlings.
Supplementary Figure 10. PB induced RD29a, RD29b and MAKKK18 highly expression.
Supplementary Figure 11. PB-induced intron retention in SR and SR-like subfamily proteins.
Supplementary Figure 12. Comparison of intron retention intensity of genes in *sr45* and WT seedlings.
Supplementary Figure 13. *in silico* study showed PB binding to PYR/PYL proteins.
Supplementary Figure 14. Yeast two hybrid assay.
Supplementary Figure 15. PB affected splicing of PP2C and SnRK2 genes differently.
Supplementary Figure 16. PB treatment induced HAB1.2 isoform high expression.
Supplementary Figure 17. Effect of PB on different ecotypes and species of plants.
Supplementary Table 1. Docking results with AutoDock 4.2.
Supplementary Table 2. Information for primers used in this paper.
Materials and Methods for Supplementary Data

References

Ali, G.S., Golovkin, M., and Reddy, A.S. (2003). Nuclear localization and in vivo dynamics of a plant-specific serine/arginine-rich protein. Plant J **36,** 883-893.

Ali, G.S., Palusa, S.G., Golovkin, M., Prasad, J., Manley, J.L., and Reddy, A.S. (2007). Regulation of plant developmental processes by a novel splicing factor. PLoS One **2,** e471.

Aouida, M., Kim, K., Shaikh, A.R., Pardo, J.M., Eppinger, J., Yun, D.J., Bressan, R.A., and Narasimhan, M.L. (2013). A Saccharomyces cerevisiae assay system to investigate ligand/AdipoR1 interactions that lead to cellular signaling. PLoS One **8,** e65454.

Bardou, F., Ariel, F., Simpson, C.G., Romero-Barrios, N., Laporte, P., Balzergue, S., Brown, J.W., and Crespi, M. (2014). Long noncoding RNA modulates alternative splicing regulators in Arabidopsis. Dev Cell **30,** 166-176.

Barta, A., Kalyna, M., and Reddy, A.S. (2010). Implementing a rational and consistent nomenclature for serine/arginine-rich protein splicing factors (SR proteins) in plants. Plant Cell **22,** 2926-2929.

Bauer, H., Ache, P., Lautner, S., Fromm, J., Hartung, W., Al-Rasheid, K.A., Sonnewald, S., Sonnewald, U., Kneitz, S., Lachmann, N., Mendel, R.R., Bittner, F., Hetherington, A.M., and Hedrich, R. (2013). The stomatal response to reduced relative humidity requires guard cell-autonomous ABA synthesis. Curr Biol **23,** 53-57.

Bonnal, S., Vigevani, L., and Valcarcel, J. (2012). The spliceosome as a target of novel antitumour drugs. Nat Rev Drug Discov **11,** 847-859.

Brooks, A.N., Yang, L., Duff, M.O., Hansen, K.D., Park, J.W., Dudoit, S., Brenner, S.E., and Graveley, B.R. (2011). Conservation of an RNA regulatory map between Drosophila and mammals. Genome Res **21,** 193-202.

Carvalho, R.F., Carvalho, S.D., and Duque, P. (2010). The plant-specific SR45 protein negatively regulates glucose and ABA signaling during early seedling development in Arabidopsis. Plant Physiol **154,** 772-783.

Chinnusamy, V., Gong, Z., and Zhu, J.K. (2008). Abscisic acid-mediated epigenetic processes in plant development and stress responses. J Integr Plant Biol **50,** 1187-1195.

Conesa, A., Madrigal, P., Tarazona, S., Gomez-Cabrero, D., Cervera, A., McPherson, A., Szczesniak, M.W., Gaffney, D.J., Elo, L.L., Zhang, X., and Mortazavi, A. (2016). A survey of best practices for RNA-seq data analysis. Genome Biol **17,** 13.

Cruz, T.M., Carvalho, R.F., Richardson, D.N., and Duque, P. (2014). Abscisic acid (ABA) regulation of Arabidopsis SR protein gene expression. Int J Mol Sci **15,** 17541-17564.

Cui, P., Zhang, S., Ding, F., Ali, S., and Xiong, L. (2014). Dynamic regulation of genome-wide pre-mRNA splicing and stress tolerance by the Sm-like protein LSm5 in Arabidopsis. Genome Biol **15,** R1.

Day, I.S., Golovkin, M., Palusa, S.G., Link, A., Ali, G.S., Thomas, J., Richardson, D.N., and Reddy, A.S. (2012). Interactions of SR45, an SR-like protein, with spliceosomal proteins and an intronic sequence: insights into regulated splicing. Plant J **71,** 936-947.

Ding, F., Cui, P., Wang, Z., Zhang, S., Ali, S., and Xiong, L. (2014). Genome-wide analysis of alternative splicing of pre-mRNA under salt stress in Arabidopsis. BMC Genomics **15,** 431.

Duan, L., Dietrich, D., Ng, C.H., Chan, P.M., Bhalerao, R., Bennett, M.J., and Dinneny, J.R. (2013). Endodermal ABA signaling promotes lateral root quiescence during salt stress in Arabidopsis seedlings. Plant Cell **25,** 324-341.

Duque, P. (2011). A role for SR proteins in plant stress responses. Plant Signal Behav **6,** 49-54.

Feng, J., Li, J., Gao, Z., Lu, Y., Yu, J., Zheng, Q., Yan, S., Zhang, W., He, H., Ma, L., and Zhu, Z. (2015). SKIP Confers Osmotic Tolerance during Salt Stress by Controlling Alternative Gene Splicing in Arabidopsis. Mol Plant **8,** 1038-1052.

Filichkin, S., Priest, H.D., Megraw, M., and Mockler, T.C. (2015). Alternative splicing in plants: directing traffic at the crossroads of adaptation and environmental stress. Curr Opin Plant Biol **24,** 125-135.

Filichkin, S.A., Priest, H.D., Givan, S.A., Shen, R., Bryant, D.W., Fox, S.E., Wong, W.K., and Mockler, T.C. (2010). Genome-wide mapping of alternative splicing in Arabidopsis thaliana. Genome Res **20,** 45-58.

Filichkin, S.A., Cumbie, J.S., Dharmawadhana, J.P., Jaiswal, P., Chang, J.H., Palusa, S.G., Reddy, A.S., Megraw, M., and Mockler, T.C. (2014). Environmental Stresses Modulate Abundance and Timing of Alternatively Spliced Circadian Transcripts in Arabidopsis. Mol Plant.

Fujii, H., and Zhu, J.K. (2009). Arabidopsis mutant deficient in 3 abscisic acid-activated protein kinases reveals critical roles in growth, reproduction, and stress. Proc Natl Acad Sci U S A **106,** 8380-8385.

Fujita, Y., Nakashima, K., Yoshida, T., Katagiri, T., Kidokoro, S., Kanamori, N., Umezawa, T., Fujita, M., Maruyama, K., Ishiyama, K., Kobayashi, M., Nakasone, S., Yamada, K., Ito, T., Shinozaki, K., and Yamaguchi-Shinozaki, K. (2009). Three SnRK2 protein kinases are the main positive regulators of abscisic acid signaling in response to water stress in Arabidopsis. Plant Cell Physiol **50,** 2123-2132.

Golovkin, M., and Reddy, A.S. (1999). An SC35-like protein and a novel serine/arginine-rich protein interact with Arabidopsis U1-70K protein. The Journal of biological chemistry **274,** 36428-36438.

Gray, S.G., and Dangond, F. (2006). Rationale for the use of histone deacetylase inhibitors as a dual therapeutic modality in multiple sclerosis. Epigenetics **1,** 67-75.

Hilscher, J., Schlotterer, C., and Hauser, M.T. (2009). A single amino acid replacement in ETC2 shapes trichome patterning in natural Arabidopsis populations. Curr Biol **19,** 1747-1751.

Howard, J.M., and Sanford, J.R. (2015). The RNAissance family: SR proteins as multifaceted regulators of gene expression. Wiley Interdiscip Rev RNA **6,** 93-110.

Huang da, W., Sherman, B.T., and Lempicki, R.A. (2009a). Bioinformatics enrichment tools: paths toward the comprehensive functional analysis of large gene lists. Nucleic Acids Res **37,** 1-13.

Huang da, W., Sherman, B.T., and Lempicki, R.A. (2009b). Systematic and integrative analysis of large gene lists using DAVID bioinformatics resources. Nat Protoc **4,** 44-57.

Ishitani, M., Xiong, L., Stevenson, B., and Zhu, J.K. (1997). Genetic analysis of osmotic and cold stress signal transduction in Arabidopsis: interactions and convergence of abscisic acid-dependent and abscisic acid-independent pathways. The Plant cell **9,** 1935-1949.

Jang, Y.H., Park, H.Y., Lee, K.C., Thu, M.P., Kim, S.K., Suh, M.C., Kang, H., and Kim, J.K. (2014). A homolog of splicing factor SF1 is essential for development and is involved in the alternative splicing of pre-mRNA in Arabidopsis thaliana. Plant J **78,** 591-603.

Jurica, M.S., and Moore, M.J. (2003). Pre-mRNA splicing: awash in a sea of proteins. Mol Cell **12,** 5-14.

Kaida, D., Motoyoshi, H., Tashiro, E., Nojima, T., Hagiwara, M., Ishigami, K., Watanabe, H., Kitahara, T., Yoshida, T., Nakajima, H., Tani, T., Horinouchi, S., and Yoshida, M. (2007). Spliceostatin A targets SF3b and inhibits both splicing and nuclear retention of pre-mRNA. Nat Chem Biol **3,** 576-583.

Kong, X., Ma, L., Yang, L., Chen, Q., Xiang, N., Yang, Y., and Hu, X. (2014). Quantitative proteomics analysis reveals that the nuclear cap-binding complex proteins arabidopsis CBP20 and CBP80 modulate the salt stress response. J Proteome Res **13,** 2495-2510.

Kotake, Y., Sagane, K., Owa, T., Mimori-Kiyosue, Y., Shimizu, H., Uesugi, M., Ishihama, Y., Iwata, M., and Mizui, Y. (2007). Splicing factor SF3b as a target of the antitumor natural product pladienolide. Nat Chem Biol **3,** 570-575.

Kuhn, J.M., Hugouvieux, V., and Schroeder, J.I. (2008). mRNA cap binding proteins: effects on abscisic acid signal transduction, mRNA processing, and microarray analyses. Curr Top Microbiol Immunol **326,** 139-150.

Labadorf, A., Link, A., Rogers, M.F., Thomas, J., Reddy, A.S., and Ben-Hur, A. (2010). Genome-wide analysis of alternative splicing in Chlamydomonas reinhardtii. BMC Genomics **11,** 114.

Laubinger, S., Sachsenberg, T., Zeller, G., Busch, W., Lohmann, J.U., Ratsch, G., and Weigel, D. (2008). Dual roles of the nuclear cap-binding complex and SERRATE in pre-mRNA splicing and microRNA processing in Arabidopsis thaliana. Proc Natl Acad Sci U S A **105,** 8795-8800.

Leviatan, N., Alkan, N., Leshkowitz, D., and Fluhr, R. (2013). Genome-wide survey of cold stress regulated alternative splicing in Arabidopsis thaliana with tiling microarray. PLoS One **8,** e66511.

Lim, G.H., Zhang, X., Chung, M.S., Lee, D.J., Woo, Y.M., Cheong, H.S., and Kim, C.S. (2010). A putative novel transcription factor, AtSKIP, is involved in abscisic acid signalling and confers salt and osmotic tolerance in Arabidopsis. New Phytol **185,** 103-113.

Luo, Y., Wang, Z., Ji, H., Fang, H., Wang, S., Tian, L., and Li, X. (2013). An Arabidopsis homolog of importin beta1 is required for ABA response and drought tolerance. Plant J **75,** 377-389.

Ma, Y., Szostkiewicz, I., Korte, A., Moes, D., Yang, Y., Christmann, A., and Grill, E. (2009). Regulators of PP2C phosphatase activity function as abscisic acid sensors. Science **324,** 1064-1068.

Mahfouz, M.M., Piatek, A., and Stewart, C.N., Jr. (2014). Genome engineering via TALENs and CRISPR/Cas9 systems: challenges and perspectives. Plant Biotechnol J **12,** 1006-1014.

Mahfouz, M.M., Li, L., Piatek, M., Fang, X., Mansour, H., Bangarusamy, D.K., and Zhu, J.K. (2012). Targeted transcriptional repression using a chimeric TALE-SRDX repressor protein. Plant molecular biology **78,** 311-321.

Mao, R., Raj Kumar, P.K., Guo, C., Zhang, Y., and Liang, C. (2014). Comparative analyses between retained introns and constitutively spliced introns in Arabidopsis thaliana using random forest and support vector machine. PLoS One **9,** e104049.

Marquez, Y., Brown, J.W., Simpson, C., Barta, A., and Kalyna, M. (2012). Transcriptome survey reveals increased complexity of the alternative splicing landscape in Arabidopsis. Genome Res **22,** 1184-1195.

McCourt, P., and Desveaux, D. (2010). Plant chemical genetics. New Phytol **185,** 15-26.

Nakaminami, K., Karlson, D.T., and Imai, R. (2006). Functional conservation of cold shock domains in bacteria and higher plants. Proc Natl Acad Sci U S A **103,** 10122-10127.

Nishida, A., Kataoka, N., Takeshima, Y., Yagi, M., Awano, H., Ota, M., Itoh, K., Hagiwara, M., and Matsuo, M. (2011). Chemical treatment enhances skipping of a mutated exon in the dystrophin gene. Nature communications **2,** 308.

O'Brien, K., Matlin, A.J., Lowell, A.M., and Moore, M.J. (2008). The biflavonoid isoginkgetin is a general inhibitor of Pre-mRNA splicing. The Journal of biological chemistry **283,** 33147-33154.

Okamoto, M., Peterson, F.C., Defries, A., Park, S.Y., Endo, A., Nambara, E., Volkman, B.F., and Cutler, S.R. (2013). Activation of dimeric ABA receptors elicits guard cell closure, ABA-regulated gene expression, and drought tolerance. Proc Natl Acad Sci U S A **110,** 12132-12137.

Palusa, S.G., Ali, G.S., and Reddy, A.S. (2007). Alternative splicing of pre-mRNAs of Arabidopsis serine/arginine-rich proteins: regulation by hormones and stresses. Plant J **49,** 1091-1107.

Pandey, R., Muller, A., Napoli, C.A., Selinger, D.A., Pikaard, C.S., Richards, E.J., Bender, J., Mount, D.W., and Jorgensen, R.A. (2002). Analysis of histone acetyltransferase and histone deacetylase families of Arabidopsis thaliana suggests functional diversification of chromatin modification among multicellular eukaryotes. Nucleic Acids Res **30,** 5036-5055.

Park, S.Y., Fung, P., Nishimura, N., Jensen, D.R., Fujii, H., Zhao, Y., Lumba, S., Santiago, J., Rodrigues, A., Chow, T.F., Alfred, S.E., Bonetta, D., Finkelstein, R., Provart, N.J., Desveaux, D., Rodriguez, P.L., McCourt, P., Zhu, J.K., Schroeder, J.I., Volkman, B.F., and Cutler, S.R. (2009). Abscisic acid inhibits type 2C protein phosphatases via the PYR/PYL family of START proteins. Science **324,** 1068-1071.

Pikaard, C.S., and Mittelsten Scheid, O. (2014). Epigenetic regulation in plants. Cold Spring Harb Perspect Biol **6,** a019315.

Piskurewicz, U., Jikumaru, Y., Kinoshita, N., Nambara, E., Kamiya, Y., and Lopez-Molina, L. (2008). The gibberellic acid signaling repressor RGL2 inhibits Arabidopsis seed germination by stimulating abscisic acid synthesis and ABI5 activity. Plant Cell **20,** 2729-2745.

Reddy, A.S., and Shad Ali, G. (2011). Plant serine/arginine-rich proteins: roles in precursor messenger RNA splicing, plant development, and stress responses. Wiley Interdiscip Rev RNA **2,** 875-889.

Reddy, A.S., Day, I.S., Gohring, J., and Barta, A. (2012). Localization and dynamics of nuclear speckles in plants. Plant Physiol **158,** 67-77.

Reddy, A.S., Marquez, Y., Kalyna, M., and Barta, A. (2013). Complexity of the alternative splicing landscape in plants. Plant Cell **25,** 3657-3683.

Ren, X., Chen, Z., Liu, Y., Zhang, H., Zhang, M., Liu, Q., Hong, X., Zhu, J.K., and Gong, Z. (2010). ABO3, a WRKY transcription factor, mediates plant responses to abscisic acid and drought tolerance in Arabidopsis. Plant J **63,** 417-429.

Rymond, B. (2007). Targeting the spliceosome. Nature chemical biology **3,** 533-535.

Saez, A., Apostolova, N., Gonzalez-Guzman, M., Gonzalez-Garcia, M.P., Nicolas, C., Lorenzo, O., and Rodriguez, P.L. (2004). Gain-of-function and loss-of-function phenotypes of the protein phosphatase 2C HAB1 reveal its role as a negative regulator of abscisic acid signalling. Plant J **37,** 354-369.

Santiago, J., Dupeux, F., Round, A., Antoni, R., Park, S.Y., Jamin, M., Cutler, S.R., Rodriguez, P.L., and Marquez, J.A. (2009). The abscisic acid receptor PYR1 in complex with abscisic acid. Nature **462,** 665-668.

Shinozaki, K., and Yamaguchi-Shinozaki, K. (2007). Gene networks involved in drought stress response and tolerance. J Exp Bot **58,** 221-227.

Soret, J., Bakkour, N., Maire, S., Durand, S., Zekri, L., Gabut, M., Fic, W., Divita, G., Rivalle, C., Dauzonne, D., Nguyen, C.H., Jeanteur, P., and Tazi, J. (2005). Selective modification of alternative splicing by indole derivatives that target serine-arginine-rich protein splicing factors. Proc Natl Acad Sci U S A **102,** 8764-8769.

Springer, N.M., Li, Q., and Lisch, D. (2016). Creating order from chaos: epigenome dynamics in plants with complex genomes. Plant Cell.

Staiger, D., and Brown, J.W. (2013). Alternative splicing at the intersection of biological timing, development, and stress responses. Plant Cell **25,** 3640-3656.

Szarzynska, B., Sobkowiak, L., Pant, B.D., Balazadeh, S., Scheible, W.R., Mueller-Roeber, B., Jarmolowski, A., and Szweykowska-Kulinska, Z. (2009). Gene structures and processing of Arabidopsis thaliana HYL1-dependent pri-miRNAs. Nucleic Acids Res **37,** 3083-3093.

Tanabe, N., Yoshimura, K., Kimura, A., Yabuta, Y., and Shigeoka, S. (2007). Differential expression of alternatively spliced mRNAs of Arabidopsis SR protein homologs, atSR30 and atSR45a, in response to environmental stress. Plant Cell Physiol **48,** 1036-1049.

Tillemans, V., Leponce, I., Rausin, G., Dispa, L., and Motte, P. (2006). Insights into nuclear organization in plants as revealed by the dynamic distribution of Arabidopsis SR splicing factors. Plant Cell **18,** 3218-3234.

Trapnell, C., Pachter, L., and Salzberg, S.L. (2009). TopHat: discovering splice junctions with RNA-Seq. Bioinformatics **25,** 1105-1111.

Umezawa, T., Sugiyama, N., Mizoguchi, M., Hayashi, S., Myouga, F., Yamaguchi-Shinozaki, K., Ishihama, Y., Hirayama, T., and Shinozaki, K. (2009). Type 2C protein phosphatases directly regulate abscisic acid-activated protein kinases in Arabidopsis. Proc Natl Acad Sci U S A **106,** 17588-17593.

Vlad, F., Rubio, S., Rodrigues, A., Sirichandra, C., Belin, C., Robert, N., Leung, J., Rodriguez, P.L., Lauriere, C., and Merlot, S. (2009). Protein phosphatases 2C regulate the activation of the Snf1-related kinase OST1 by abscisic acid in Arabidopsis. Plant Cell **21,** 3170-3184.

Wang, P., Xue, L., Batelli, G., Lee, S., Hou, Y.J., Van Oosten, M.J., Zhang, H., Tao, W.A., and Zhu, J.K. (2013). Quantitative phosphoproteomics identifies SnRK2 protein kinase substrates and reveals the effectors of abscisic acid action. Proc Natl Acad Sci U S A **110,** 11205-11210.

Wang, X., Wu, F., Xie, Q., Wang, H., Wang, Y., Yue, Y., Gahura, O., Ma, S., Liu, L., Cao, Y., Jiao, Y., Puta, F., McClung, C.R., Xu, X., and Ma, L. (2012). SKIP is a component of the spliceosome linking alternative splicing and the circadian clock in Arabidopsis. Plant Cell **24,** 3278-3295.

Wang, Z., Ji, H., Yuan, B., Wang, S., Su, C., Yao, B., Zhao, H., and Li, X. (2015). ABA signalling is fine-tuned by antagonistic HAB1 variants. Nat Commun **6,** 8138.

Will, C.L., and Luhrmann, R. (2011). Spliceosome structure and function. Cold Spring Harb Perspect Biol **3**.

Xing, D., Wang, Y., Hamilton, M., Ben-Hur, A., and Reddy, A.S. (2015). Transcriptome-Wide Identification of RNA Targets of Arabidopsis SERINE/ARGININE-RICH45 Uncovers the Unexpected Roles of This RNA Binding Protein in RNA Processing. Plant Cell **27,** 3294-3308.

Yamaguchi-Shinozaki, K., and Shinozaki, K. (1994). A novel cis-acting element in an Arabidopsis gene is involved in responsiveness to drought, low-temperature, or high-salt stress. The Plant cell **6,** 251-264.

Zhan, X., Qian, B., Cao, F., Wu, W., Yang, L., Guan, Q., Gu, X., Wang, P., Okusolubo, T.A., Dunn, S.L., Zhu, J.K., and Zhu, J. (2015). An Arabidopsis PWI and RRM motif-containing protein is critical for pre-mRNA splicing and ABA responses. Nat Commun **6,** 8139.

Zhang, X.N., and Mount, S.M. (2009). Two alternatively spliced isoforms of the Arabidopsis SR45 protein have distinct roles during normal plant development. Plant Physiol **150,** 1450-1458.

Zhu, J.K. (2002). Salt and drought stress signal transduction in plants. Annu Rev Plant Biol **53,** 247-273.

Zimmermann, P., Hirsch-Hoffmann, M., Hennig, L., and Gruissem, W. (2004). GENEVESTIGATOR. Arabidopsis microarray database and analysis toolbox. Plant Physiol **136,** 2621-2632.

Figure Legends:

Figure 1. Pladienolide B inhibited *Arabidopsis thaliana* seed germination and root elongation. A, Effects of different drugs on the elongation of primary root of Arabidopsis. 5-day-old Col-0 seedlings were transferred onto ½MS medium with chemicals for additional 3 days. Note: Concentration of PB different from others, green box stands for 0.5 μM, purple box stands for 1 μM, orange box stands for 5 μM. Median PR length under DMSO is indicated by the dotted line. "*" indicates statistically significant differences compared with DMSO treatment (Student's t-test, *p*-value ≤ 0.05). B, Growth inhibition of Arabidopsis seedlings by PB. 5-day-old Col-0 seedlings transferred from MS media to MS media containing DMSO, 1 and 5 μM of PB for additional 7 days, the root tip of the transferring time was shown by the red bar. On control medium, the seedlings grow well with 4 green true leaves and long roots. On 1 μM PB medium, the seedlings grow slowly with 2 yellow true leaves. On 5 μM PB medium, the seedlings totally stop growing, bar, 10 mm. C, Effects of PB on Arabidopsis seed germination. PB inhibit seed germination in a dose-dependent manner, less than half of seeds germinated after 4 days (n=100).

Figure 2. PB altered the splicing pattern of a set of genes. The cDNAs were prepared from one-week-old Arabidopsis seedlings that were treated with PB (0.5, 1, or 5 μM) for 6 or 24 h, as indicated, with DMSO as control. RT-PCR was performed using primers that flank introns. Arrowheads indicate splicing variants that changed following PB treatment, "*" indicates splice variants with unknown length. The gene structure flanking the amplified fragments and the structures of regulated variants are shown under the gel images (green arrows mark the positions of primers). Blue box, exon; line, intron; white box, 5' or 3' UTR; light blue; retained intron. The gene locus identifier is shown on the bottom. Alteration of splicing patterns in response to PB in: A, *APX3* (AT4G35800); B, *ATSEN1* (AT4G35770); C, *HAC04* (AT1G55970); D, *NADP-ME2* (AT5G11670).

Figure 3. Gene expression changed by PB corresponding to stress responses. A, A heatmap was generated by mapping the up-regulated genes at 6 h treatment to the microarray database using Genevestigator. The heatmap indicates that a great number of these genes are up-regulated (colored red) by ABA, drought and salt stress. B, Functional categorization (biological process) of differentially expressed genes at 6 h treatment. The top 25 enriched pathways are shown.

Figure 4. PB induced intron retention. A and B, Comparison of intron retention between control and PB treatments. The RPKM values for the exons and introns were plotted. The expression of introns, but not exons, in PB 6h treatments showed a global up-regulation (A). The expression of introns, but not exons, in PB 6h treatments showed a global up-regulation (B). C and D, Intron retention events hugely increased in the PB-treated samples, while the other AS events (including alternative 5'SSs, 3'SSs, and exon skipping) decreased in the PB-treated 6h (C) and 24h (D) samples.

Figure 5. Genes with perturbed splicing in PB treatments are associated with stress responses. A, A two-dimension representation of the relationship between the genes with perturbed splicing in PB at 6 h treatment and their corresponding functional annotation. The top 40 functional annotations were ordered according to their enrichment scores and selected for the two-dimension view indicating that the significant abnormal splicing was enriched in the

response-to-abiotic-stress category. B, Functional category of genes with perturbed splicing in the 6 h treatment. Top 20 categories that were ordered by the enrichment scores were selected.

Figure 6. Genes associated with stress responses show perturbed splicing in response to PB treatment. The cDNAs were prepared from one week old Arabidopsis seedlings which were treated by 5 μM PB for6h, DMSO as control. Gene structure and intron retention of interesting regions from 10 genes were shown in IGV program, validation of intron retention of each gene was performed by RT-PCR using intron-flanking primers, with result shown on the right. The red bar in the IGV program snapshot represents the target amplification region. C6, DMSO 6h treatment; P6, PB 6h treatment.

Figure 7. PB induced RD29A-LUC expression and promoted stomatal aperture closure. A, B, Ten-day-old *RD29A-LUC* transgenic seedlings were treated with 5 μM PB for 6 h, then sprayed with D-luciferase and observed by CCD camera. DMSO was used as the negative control and 100 μM ABA was used as positive control. A, bioluminescence of *RD29A-LUC* transgenic plants, bright-field image is shown below. B, bioluminescence intensities of RD29A-LUC seedling in each well were measured by TECAN Ultra 96 microplate reader. C-I, Leaves of 2- to 3-week-old Arabidopsis and fava bean were treated in opening solution for about 2.5 h and then transferred into opening solution with 20 μM PB for 4 h. DMSO and ABA were used as negative and positive controls, respectively. Arabidopsis stomata cells kept in opening solution with DMSO (C), ABA (D), and PB (E). F, Measurement of stomatal aperture in Arabidopsis leaves, three replicates and about 100 stomata in each replicate were measured. Stomatal cells of fava bean in solution with DMSO (G), ABA (H), and PB (I). J, Measurement of stomatal aperture in fava bean leaves, three replicates and about 100 stomata in each replicate were measured. Values are means ± SE, "*" indicates statistically significant differences compared with DMSO treatment (Student's *t*-test, *P<0.05).

Figure 8. PB induced formation of SR45:GFP nuclear speckles and *sr45* mutant was hypersensitive to PB. A-H, One-week-old *35S:SR45:GFP* and *NSR:NSR:GFP* transgenic seedlings were treated with DMSO (control) or 5 μM PB for 24 h. A, GFP signal in the elongation zone of a *35S:SR45:GFP* root in control conditions. B, GFP signal in the elongation zone of a *35S:SR45:GFP* root in PB treatment. C, GFP signal in the elongation zone of a *NSR:NSR:GFP* root in control conditions. B, GFP signal in the elongation zone of a *35S:SR45:GFP* root in PB treatment. E, close up of nuclei of elongation zone cells from DMSO-treated *35S:SR45:GFP* transgenic plants. F, close up of nuclei of elongation zone cells from 5 μM PB-treated *35S:SR45:GFP* transgenic plants, nuclear speckles formed in the nuclei. G, close up of nuclei of elongation zone cells from DMSO-treated *NSR:NSR:GFP* transgenic plants. H, close up of nuclei elongation zone cells from 5 μM PB-treated *NSR:NSR:GFP* transgenic plants. H, close up of nuclei elongation zone cells from 5 μM PB treated *NSR:NSR:GFP* transgenic plants. I and J, 5 day old Arabidopsis Col (0) wild type and *sr45-1* mutant seedlings were transferred onto ½ MS medium with 0.2 μM for 4 days. I, comparison of primary root elongation rate of Col (0) and *sr45-1* mutant on 0.2 μM PB plates, the root tip of the transferring time was shown by the red bar. J, Col (0) plants keep more 35% of elongation rate when compared to its elongation rate on DMSO plate , whereas *sr45-1* almost stop growing with elongation rate less than 5%, compared with its elongation rate on DMSO plate. Values are means ± SE, "*" indicates statistically significant differences compared with DMSO treatment (Student's *t* test, **P*<0.05). Scale bar 100 μm in A-D, 5 μm in E-H, and 10 mm in I.

Figure 9. Plants with reduced ABA sensitivity are partially resistant to PB. A, abi1-1C mutant is partially resistant to PB in seedling establishment compared to wt. Quantification of

seedling establishment (seedlings developing a first pair of true leaves) was performed on MS plates supplemented with DMSO (Control, white bars), 1μM PB (black bars) or 1μM ABA (grey bars) 7 days after sown. Values are average of 3 independent experiments ±SD (n>100). * indicates a p-value≤0.05 by t-test compared to wt under the same treatment. B, Photograph of representative seedlings from A. C, The *abi1-1C* and *snrk2.2/2.3/2.6* mutants are partially resistant to PB in seed germination. Seeds were stratified for 72h in cold and seed germination (radicle emergence) was calculated 48h after transfer the seeds to the growth conditions. Values are average of 3 independent experiments ±SD (n>100). * indicates a p-value≤0.05 by t-test compared to wt under the same treatment. Seeds were sown on MS plates supplemented with DMSO (Control, white bars), 1μM PB (black bars) and 10μM ABA (grey bars). D, Plants with reduced sensitivity to ABA are partially resistant to PB in root growth. Seedlings grown in vertical on MS plates for 3 days were transferred to MS plates containing DMSO (Control, white bars), 1μM PB (black bars) or 10μM ABA (grey bars). Root length was calculated with ImageJ 7 days after the transfer. Values are average of 3 independent experiments ±SD (n>12). * indicates a p-value≤0.05 by t-test compared to wt under the same treatment. E, Photograph of representative seedlings from D.

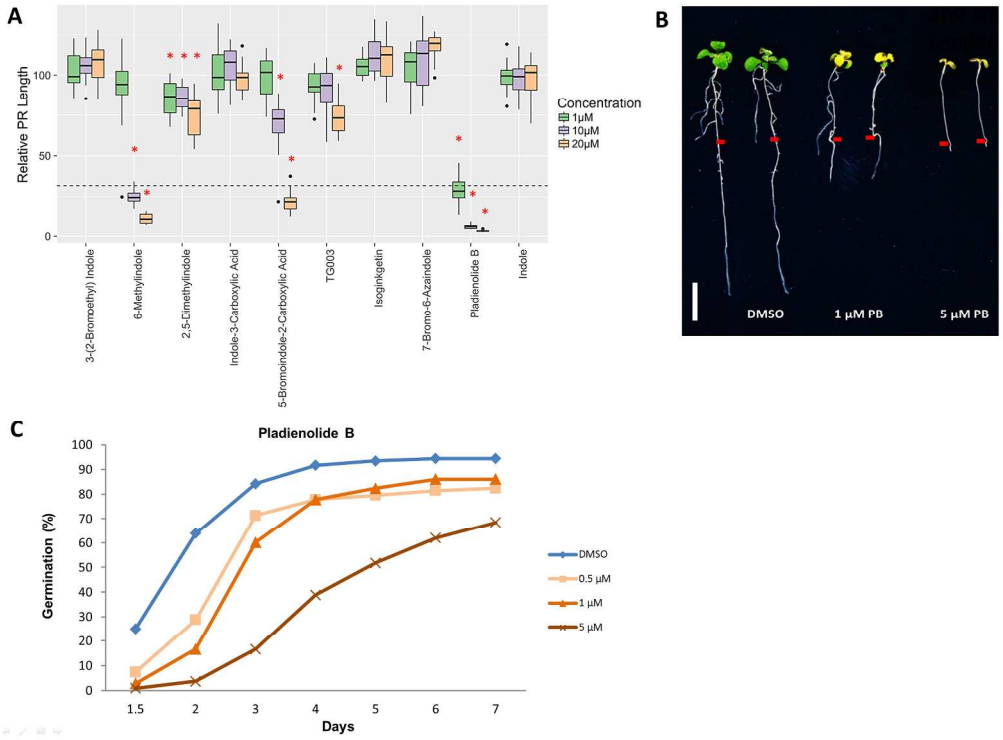

Figure 1. Pladienolide B inhibited Arabidopsis thaliana seed germination and root elongation. A, Effects of different drugs on the elongation of primary root of Arabidopsis. 5-day-old Col-0 seedlings were transferred onto ½MS medium with chemicals for additional 3 days. Note: Concentration of PB different from others, green box stands for 0.5 μM, purple box stands for 1 μM, orange box stands for 5 μM. Median PR length under DMSO is indicated by the dotted line. "*" indicates statistically significant differences compared with DMSO treatment (Student's t-test, p-value ≤ 0.05). B, Growth inhibition of Arabidopsis seedlings by PB. 5-day-old Col-0 seedlings transferred from MS media to MS media containing DMSO, 1 and 5 μM of PB for additional 7 days, the root tip of the transferring time was shown by the red bar. On control medium, the seedlings grow well with 4 green true leaves and long roots. On 1 μM PB medium, the seedlings grow slowly with 2 yellow true leaves. On 5 μM PB medium, the seedlings totally stop growing, bar, 10 mm. C, Effects of PB on Arabidopsis seed germination. PB inhibit seed germination in a dose-dependent manner, less than half of seeds germinated after 4 days (n=100).

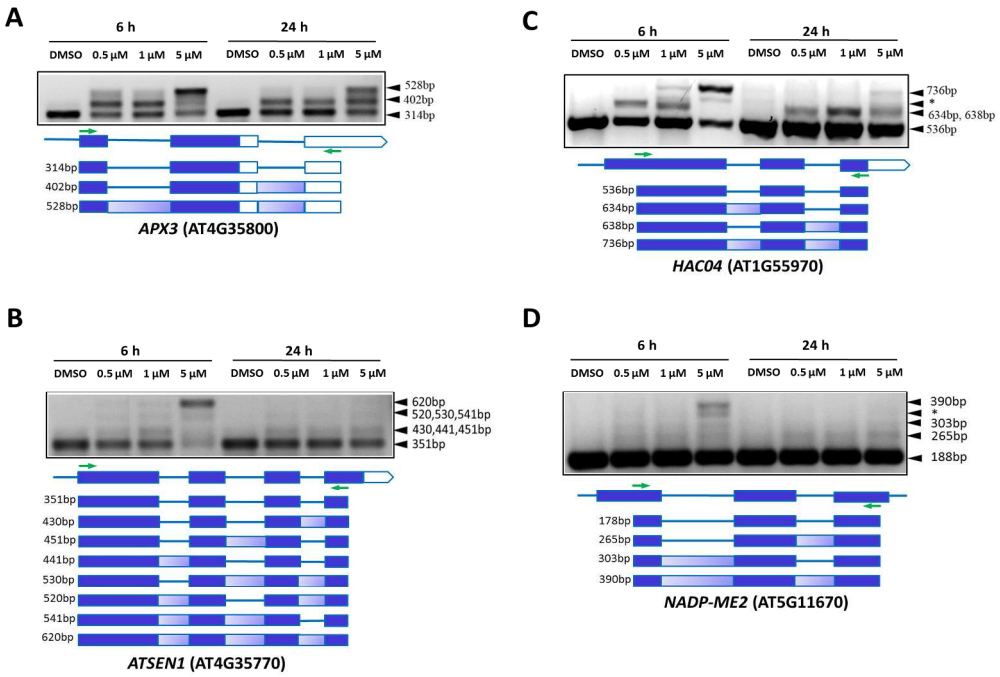

Figure 2. PB altered the splicing pattern of a set of genes. The cDNAs were prepared from one-week-old Arabidopsis seedlings that were treated with PB (0.5, 1, or 5 μM) for 6 or 24 h, as indicated, with DMSO as control. RT-PCR was performed using primers that flank introns. Arrowheads indicate splicing variants that changed following PB treatment, "*" indicates splice variants with unknown length. The gene structure flanking the amplified fragments and the structures of regulated variants are shown under the gel images (green arrows mark the positions of primers). Blue box, exon; line, intron; white box, 5′ or 3′ UTR; light blue; retained intron. The gene locus identifier is shown on the bottom. Alteration of splicing patterns in response to PB in: A, APX3 (AT4G35800); B, ATSEN1 (AT4G35770); C, HAC04 (AT1G55970); D, NADP-ME2 (AT5G11670).

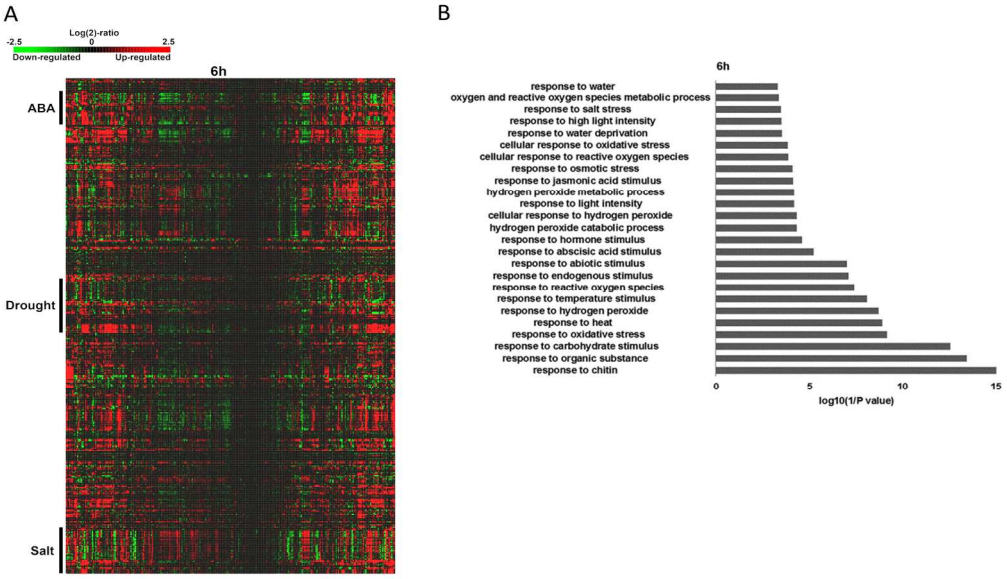

Figure 3. Gene expression changed by PB corresponding to stress responses. A, A heatmap was generated by mapping the up-regulated genes at 6 h treatment to the microarray database using Genevestigator. The heatmap indicates that a great number of these genes are up-regulated (colored red) by ABA, drought and salt stress. B, Functional categorization (biological process) of differentially expressed genes at 6 h treatment. The top 25 enriched pathways are shown.

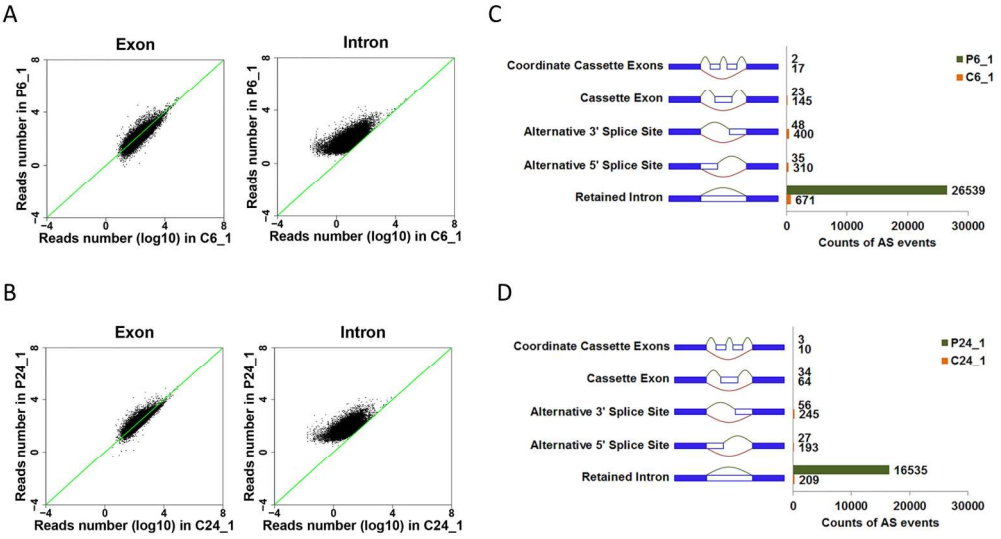

Figure 4. PB induced intron retention. A and B, Comparison of intron retention between control and PB treatments. The RPKM values for the exons and introns were plotted. The expression of introns, but not exons, in PB 6h treatments showed a global up-regulation (A). The expression of introns, but not exons, in PB 6h treatments showed a global up-regulation (B). C and D, Intron retention events hugely increased in the PB-treated samples, while the other AS events (including alternative 5′SSs, 3′SSs, and exon skipping) decreased in the PB-treated 6h (C) and 24h (D) samples.

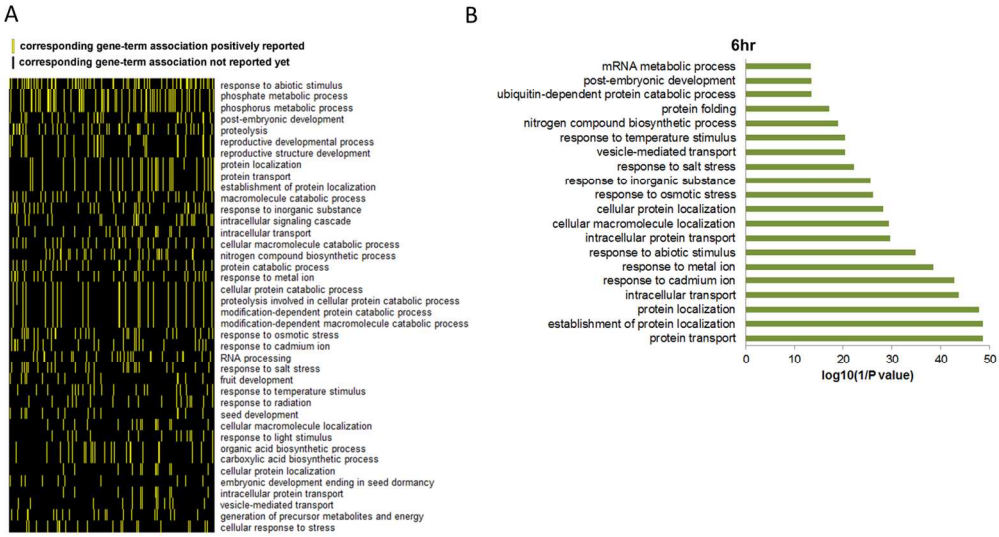

Figure 5. Genes with perturbed splicing in PB treatments are associated with stress responses. A, A two-dimension representation of the relationship between the genes with perturbed splicing in PB at 6 h treatment and their corresponding functional annotation. The top 40 functional annotations were ordered according to their enrichment scores and selected for the two-dimension view indicating that the significant abnormal splicing was enriched in the response-to-abiotic-stress category. B, Functional category of genes with perturbed splicing in the 6 h treatment. Top 20 categories that were ordered by the enrichment scores were selected.

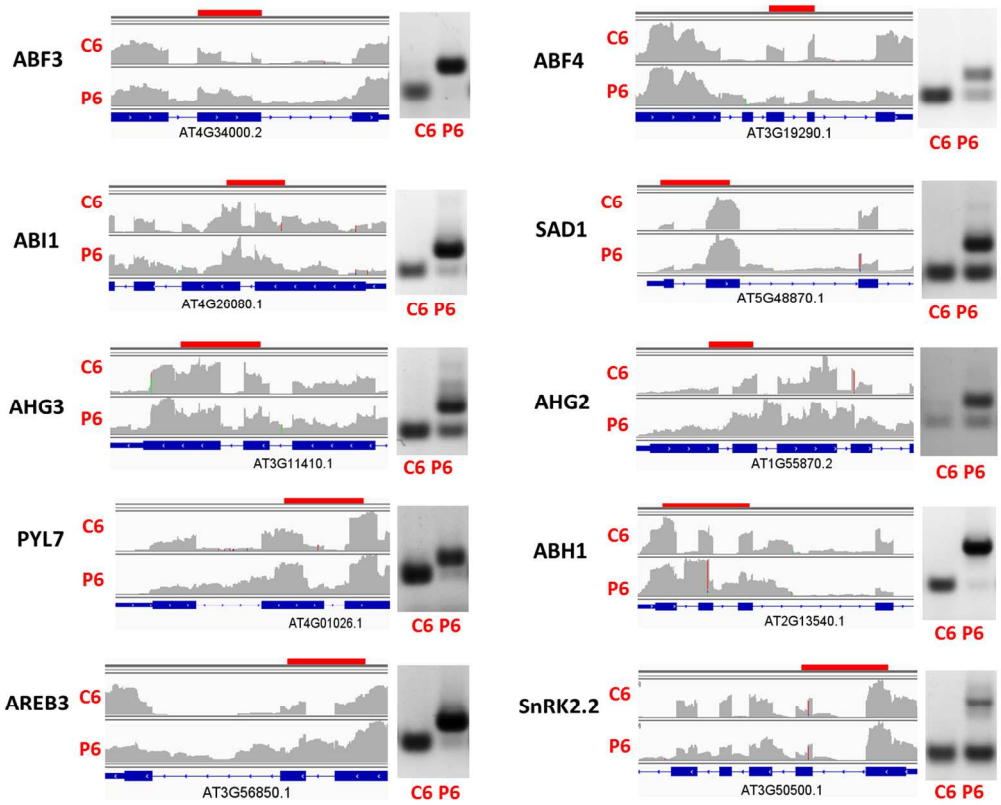

Figure 6. Genes associated with stress responses show perturbed splicing in response to PB treatment. The cDNAs were prepared from one week old Arabidopsis seedlings which were treated by 5 μM PB for6h, DMSO as control. Gene structure and intron retention of interesting regions from 10 genes were shown in IGV program, validation of intron retention of each gene was performed by RT-PCR using intron-flanking primers, with result shown on the right. The red bar in the IGV program snapshot represents the target amplification region. C6, DMSO 6h treatment; P6, PB 6h treatment.

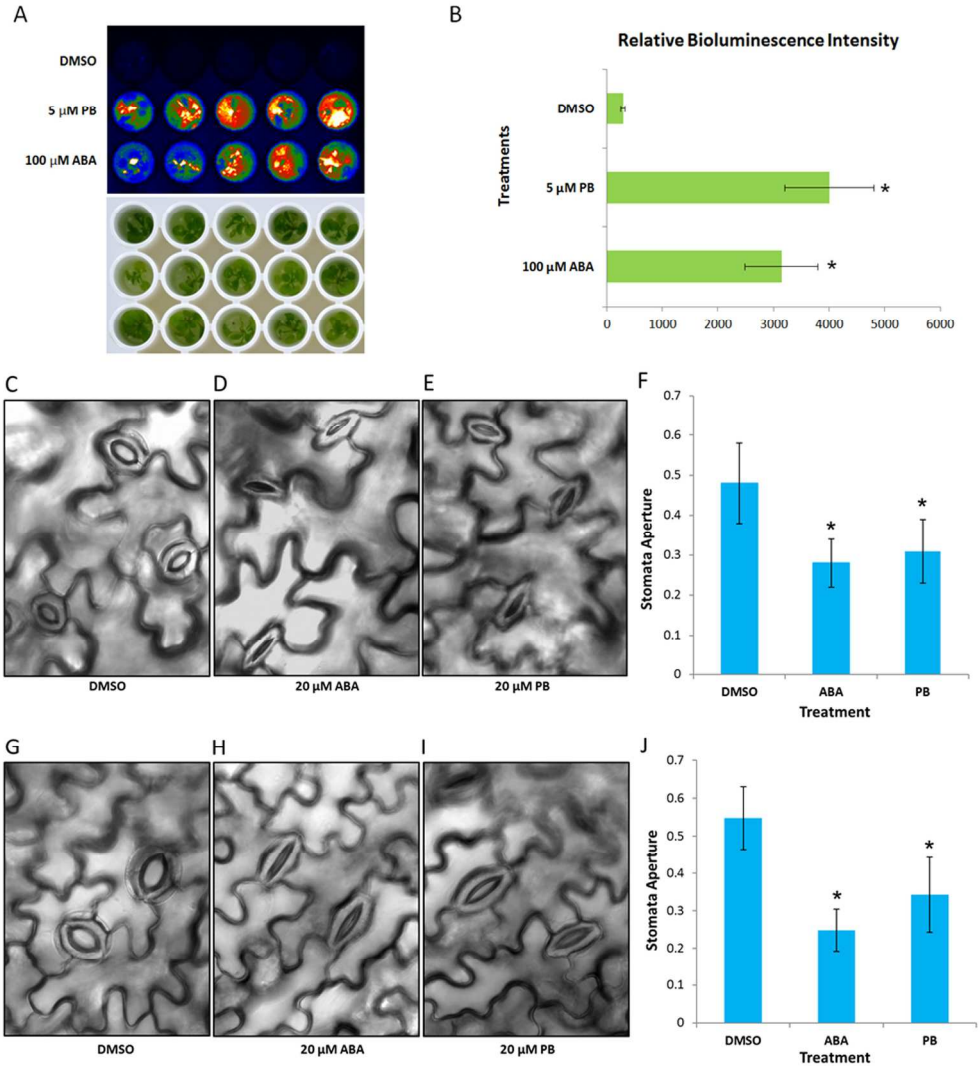

Figure 7. PB induced RD29A-LUC expression and promoted stomatal aperture closure. A, B, Ten-day-old RD29A-LUC transgenic seedlings were treated with 5 μM PB for 6 h, then sprayed with D-luciferase and observed by CCD camera. DMSO was used as the negative control and 100 μM ABA was used as positive control. A, bioluminescence of RD29A-LUC transgenic plants, bright-field image is shown below. B, bioluminescence intensities of RD29A-LUC seedling in each well were measured by TECAN Ultra 96 microplate reader. C-I, Leaves of 2- to 3-week-old Arabidopsis and fava bean were treated in opening solution for about 2.5 h and then transferred into opening solution with 20 μM PB for 4 h. DMSO and ABA were used as negative and positive controls, respectively. Arabidopsis stomata cells kept in opening solution with DMSO (C), ABA (D), and PB (E). F, Measurement of stomatal aperture in Arabidopsis leaves, three replicates and about 100 stomata in each replicate were measured. Stomatal cells of fava bean in solution with DMSO (G), ABA (H), and PB (I). J, Measurement of stomatal aperture in fava bean leaves, three replicates and about 100 stomata in each replicate were measured. Values are means ± SE, "*" indicates statistically significant differences compared with DMSO treatment (Student's t-test, *P<0.05).

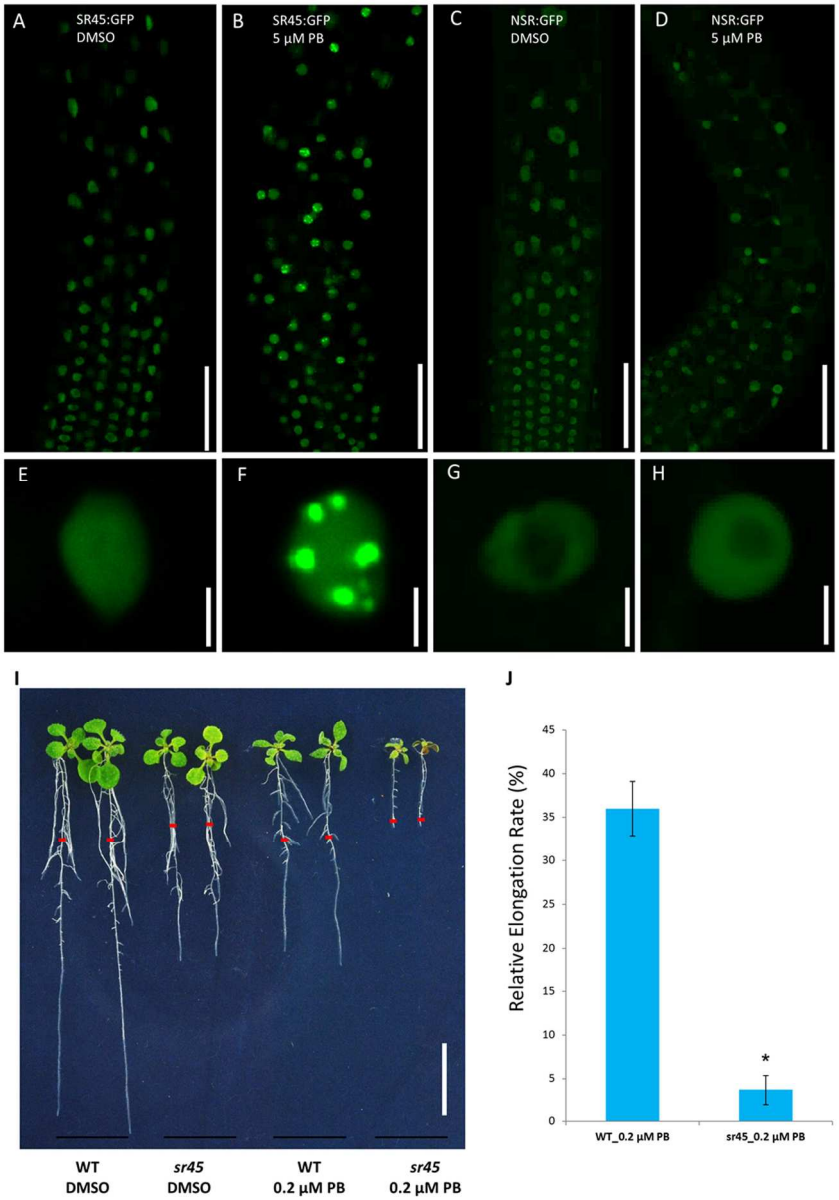

Figure 8. PB induced formation of SR45:GFP nuclear speckles and sr45 mutant was hypersensitive to PB. A-H, One-week-old 35S:SR45:GFP and NSR:NSR:GFP transgenic seedlings were treated with DMSO (control) or 5 μM PB for 24 h. A, GFP signal in the elongation zone of a 35S:SR45:GFP root in control conditions. B, GFP signal in the elongation zone of a 35S:SR45:GFP root in PB treatment. C, GFP signal in the elongation zone of a NSR:NSR:GFP root in control conditions. B, GFP signal in the elongation zone of a 35S:SR45:GFP root in PB treatment. E, close up of nuclei of elongation zone cells from DMSO-treated 35S:SR45:GFP transgenic plants. F, close up of nuclei of elongation zone cells from 5 μM PB-treated 35S:SR45:GFP transgenic plants, nuclear speckles formed in the nuclei. G, close up of nuclei of elongation zone cells from DMSO-treated NSR:NSR:GFP transgenic plants. H, close up of nuclei elongation zone cells from 5 μM PB-treated NSR:NSR:GFP transgenic plants. H, close up of nuclei elongation zone cells from 5 μM PB treated NSR:NSR:GFP transgenic plants. I and J, 5 day old Arabidopsis Col (0) wild type and sr45-1 mutant seedlings were transferred onto ½ MS medium with 0.2 μM for 4 days. I, comparison of primary root elongation rate of Col (0) and sr45-1 mutant on 0.2 μM PB plates, the root tip of the transferring time was

shown by the red bar. J, Col (0) plants keep more 35% of elongation rate when compared to its elongation rate on DMSO plate , whereas sr45-1 almost stop growing with elongation rate less than 5%, compared with its elongation rate on DMSO plate. Values are means ± SE, "*" indicates statistically significant differences compared with DMSO treatment (Student's t test, *P<0.05). Scale bar 100 μm in A-D, 5 μm in E-H, and 10 mm in I.

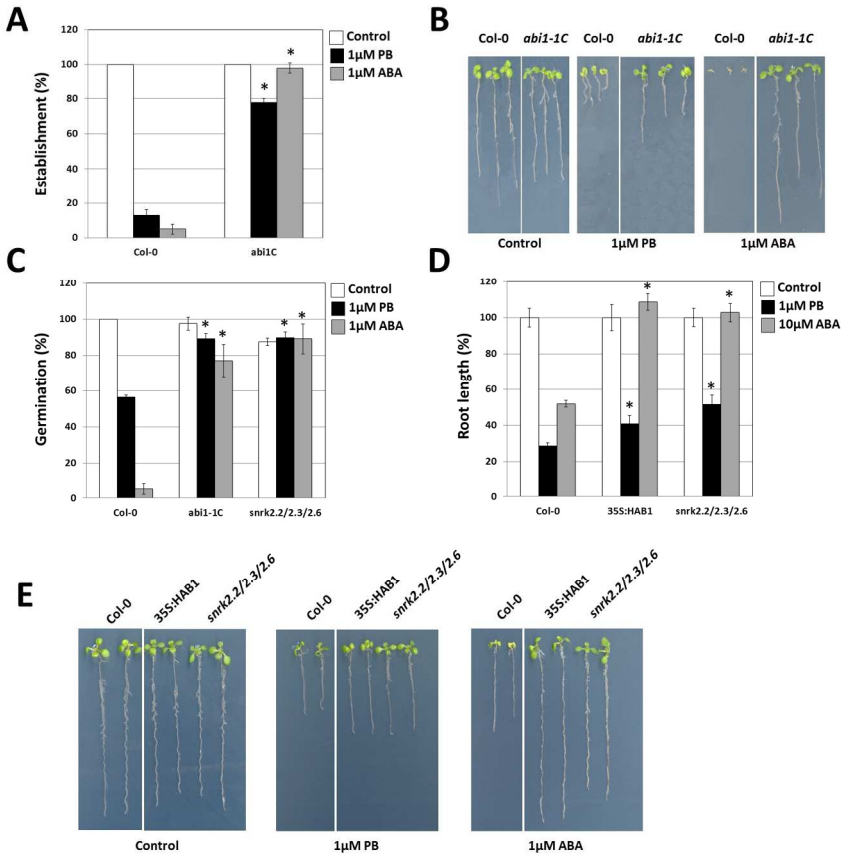

Figure 9. Plants with reduced ABA sensitivity are partially resistant to PB. A, abi1-1C mutant is partially resistant to PB in seedling establishment compared to wt. Quantification of seedling establishment (seedlings developing a first pair of true leaves) was performed on MS plates supplemented with DMSO (Control, white bars), 1µM PB (black bars) or 1µM ABA (grey bars) 7 days after sown. Values are average of 3 independent experiments ±SD (n>100). * indicates a p-value≤0.05 by t-test compared to wt under the same treatment. B, Photograph of representative seedlings from A. C, The abi1-1C and snrk2.2/2.3/2.6 mutants are partially resistant to PB in seed germination. Seeds were stratified for 72h in cold and seed germination (radicle emergence) was calculated 48h after transfer the seeds to the growth conditions. Values are average of 3 independent experiments ±SD (n>100). * indicates a p-value≤0.05 by t-test compared to wt under the same treatment. Seeds were sown on MS plates supplemented with DMSO (Control, white bars), 1µM PB (black bars) and 10µM ABA (grey bars). D, Plants with reduced sensitivity to ABA are partially resistant to PB in root growth. Seedlings grown in vertical on MS plates for 3 days were transferred to MS plates containing DMSO (Control, white bars), 1µM PB (black bars) or 10µM ABA (grey bars). Root length was calculated with ImageJ 7 days after the transfer. Values are average of 3 independent experiments ±SD (n>12). * indicates a p-value≤0.05 by t-test compared to wt under the same treatment. E, Photograph of representative seedlings from D.

508x457mm (96 x 96 DPI)

A

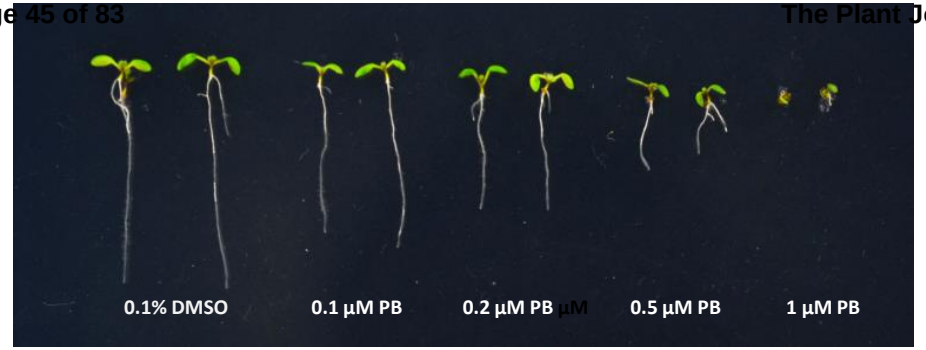
0.1% DMSO
0.1 µM PB
0.2 µM PB
0.5 µM PB
1 µM PB

B

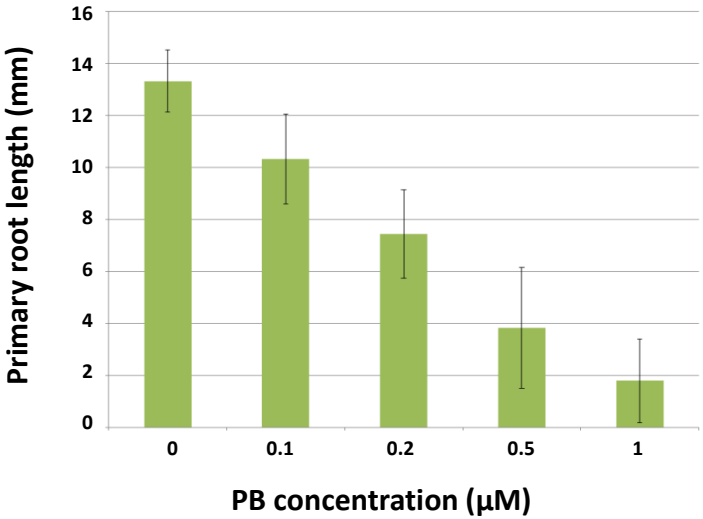
Primary root length (mm)
16
14
12
10
8
6
4
2
0
0
0.1
0.2
0.5
1
PB concentration (µM)

C

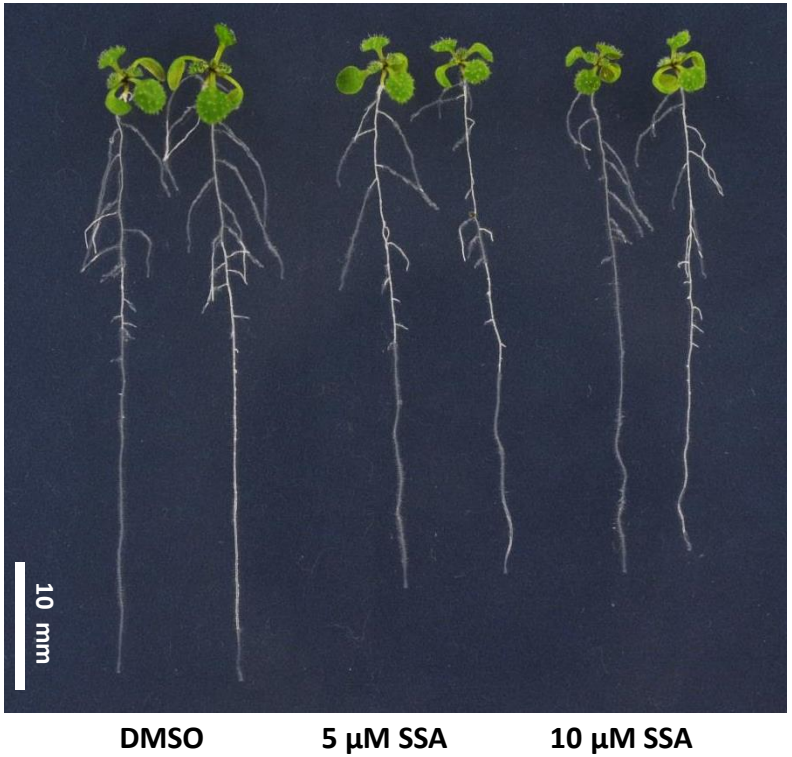
10 mm
DMSO
5 µM SSA
10 µM SSA

Supplementary Figure 1. Effects of PB and SSA on root elongation rate. A, Col-0 seedlings germinated on MS media containing 0, or 0.1, 0.2, 0.5, 1 µM of PB for 7 days, PB inhibited Arabidopsis root elongation rate in a dose-dependent manner. B, Primary root length of seedlings germinated on different concentrations of PB. C, 5 day old Col-0 Arabidopsis seedlings were transferred onto ½ MS medium with 5, 10 µM SSA for 4 days. SSA exhibited weak effect on Arabidopsis growth.

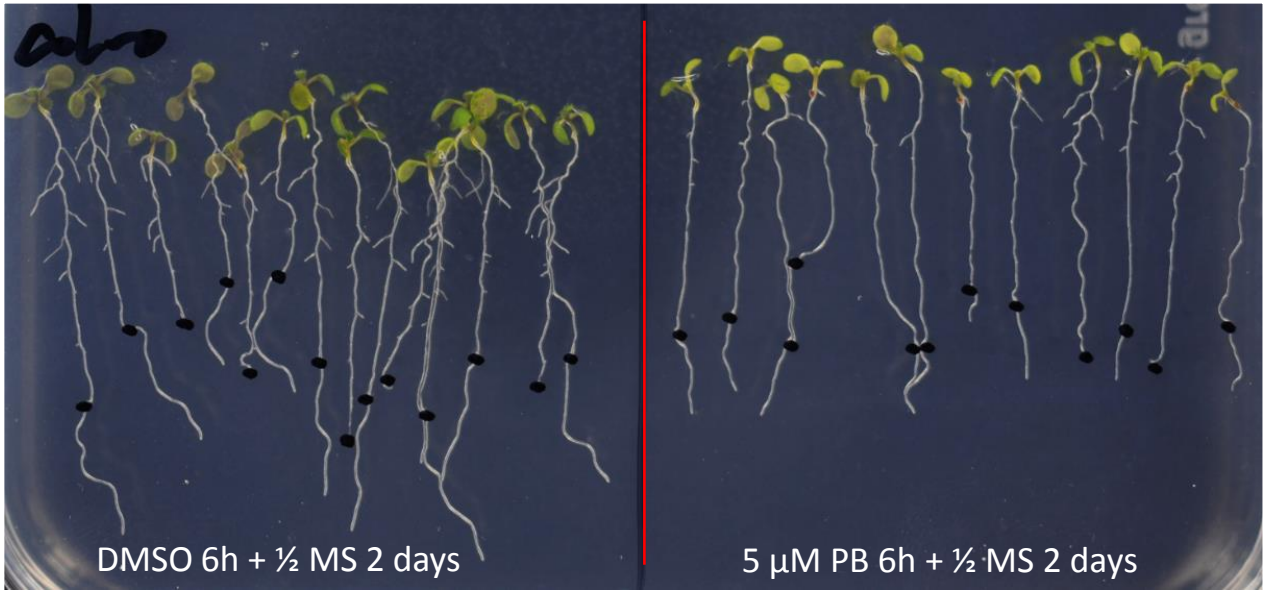
DMSO 6h + ½ MS 2 days
5 µM PB 6h + ½ MS 2 days

Supplementary Figure 2. Arabidopsis seedlings recovered from PB treatment.

Comparison of Col-0 seedlings recover from DMSO 6h treatment (left) and 5 µM PB 6h treatment (right). The seedlings treated by 5 µM PB kept growing after transferred onto half MS plate, though the growth rate is slower than that treated in DMSO. Black dots mark the positions of root tips when transferring.

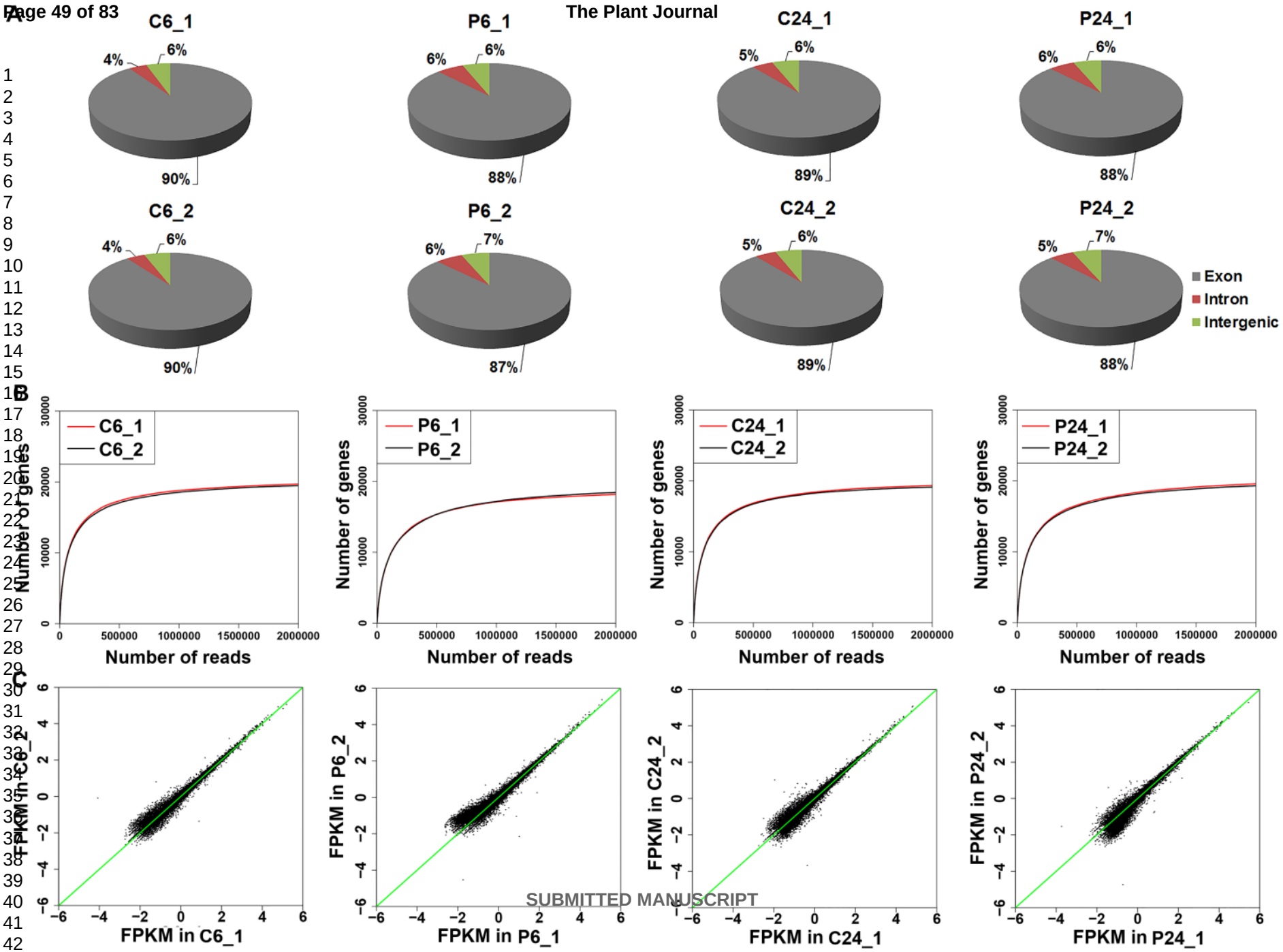

Supplementary Figure 3. High quality of RNA-seq data. A, Distribution of the RNA-seq reads along annotated Arabidopsis genomic features. Among the mapped reads more than 80% of reads map to the annotated exon, about 7% to intergenic region and 4-6% to intron. B, Saturation curve for gene detection in Control and PB-treated samples. Randomly sampled reads were plotted against the expressed genes. C, Comparison of gene expression between the two replicates. The FPKM values were plotted.

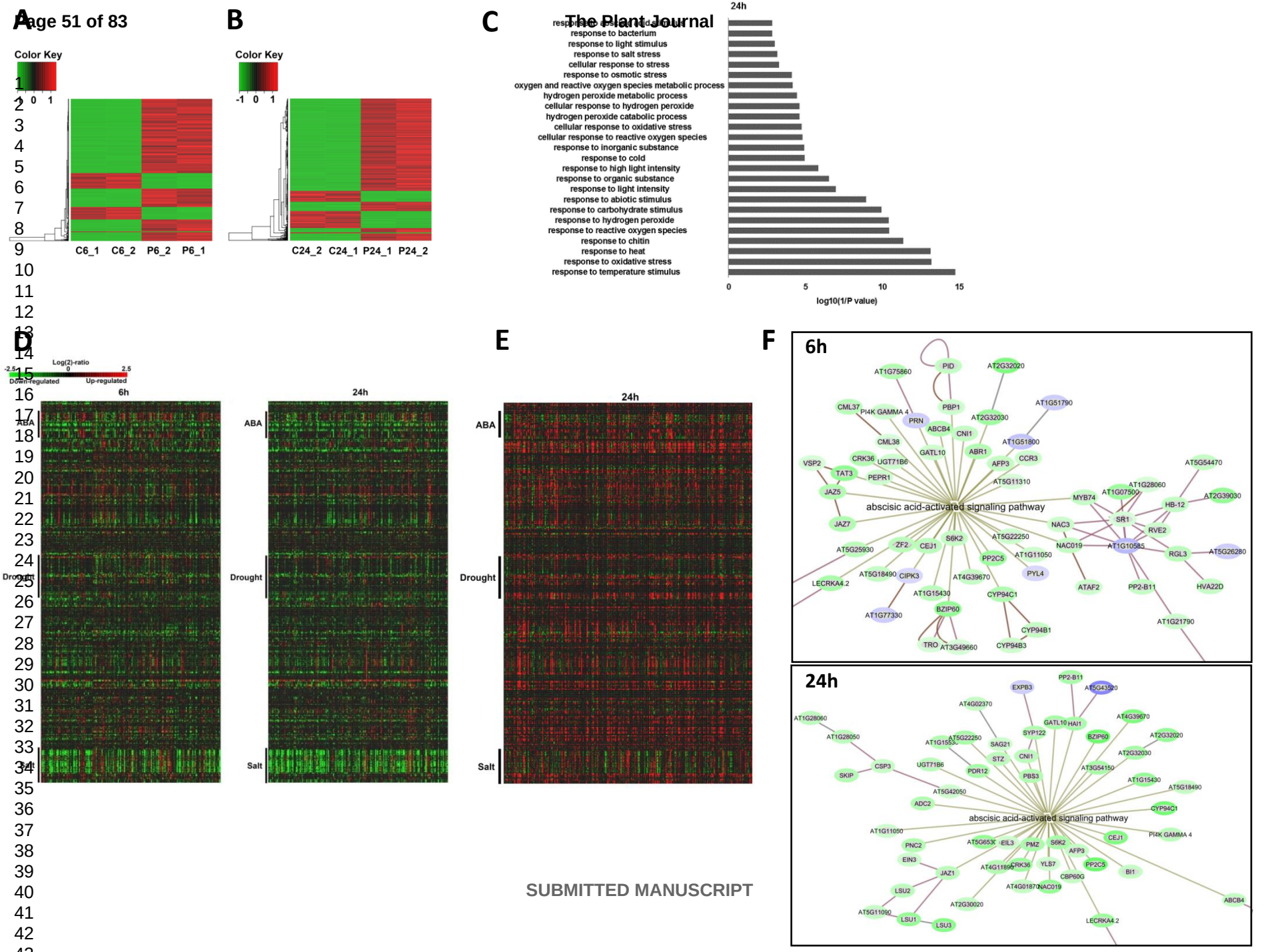
A
Color Key
-1 0 1
C6_1 C6_2 P6_2 P6_1
B
Color Key
-1 0 1
C24_2 C24_1 P24_1 P24_2
C
24h
response to bacterium
response to light stimulus
response to salt stress
cellular response to stress
response to osmotic stress
oxygen and reactive oxygen species metabolic process
hydrogen peroxide metabolic process
cellular response to hydrogen peroxide
hydrogen peroxide catabolic process
cellular response to oxidative stress
cellular response to reactive oxygen species
response to inorganic substance
response to cold
response to high light intensity
response to organic substance
response to light intensity
response to abiotic stimulus
response to carbohydrate stimulus
response to hydrogen peroxide
response to reactive oxygen species
response to chitin
response to heat
response to oxidative stress
response to temperature stimulus
0 5 10 15
log10(1/P value)
D
Log(2)-ratio
-2.5 0 2.5
Down-regulated
Up-regulated
6h
24h
ABA
Drought
Salt
E
24h
ABA
Drought
Salt
F
6h
abscisic acid-activated signaling pathway
24h
abscisic acid-activated signaling pathway

Supplementary Figure 4. Gene expression changed by PB corresponding to stress responses. A, The clustering of gene expression levels between control and treatments. By clustering, 806 significantly differentially expressed genes in 6h treatment (A) and 893 significantly differentially expressed genes in 24h treatment (B) were detected. C, Functional categorization (biological process) of differentially expressed genes in 24h treatment. Top 25 enriched pathways were selected to be shown. D, heatmaps were generated by mapping the down-regulated genes in 6h/24h treatments to the microarray database using Genevestigator. The heatmap indicates that a great number of these genes are down-regulated (colored green) by ABA, drought and salt stress. E, A heatmap was generated by mapping the up-regulated genes in 24h treatment to the microarray database using Genevestigator. The heatmap indicates that many of these genes are up-regulated (colored red) by ABA, drought and salt stress. F, Differentially expressed genes in 6h/24h treatment were mapped onto abscisic acid-activated signaling network. The analysis was performed using Exploratory Gene Association Networks (EGAN) software tool. Yellow lines show the participation of the genes in abscisic acid-activated signaling pathway and brown lines show known interaction between genes connected. Green ovals represent up-regulated genes and blue ovals represent down-regulated genes.

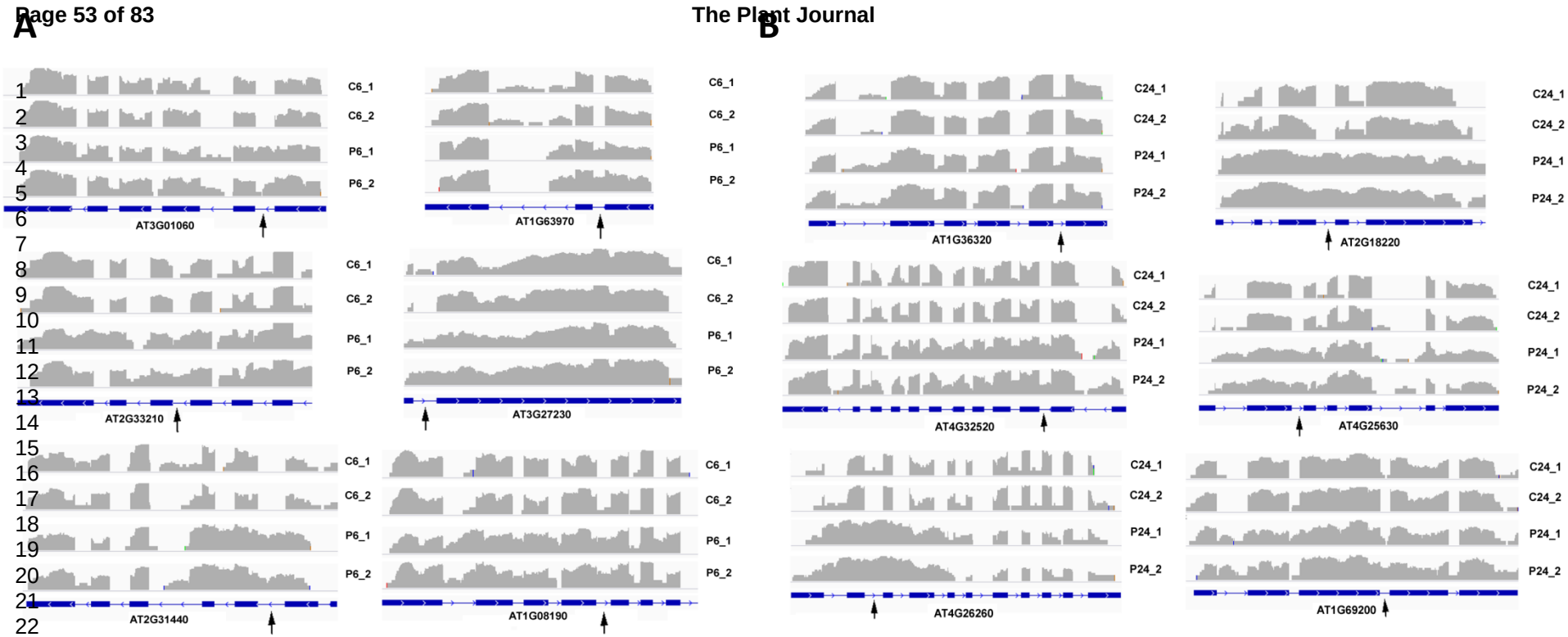
A
B
C6_1
C6_2
P6_1
P6_2
AT3G01060
AT1G63970
AT2G33210
AT3G27230
AT2G31440
AT1G08190
C24_1
C24_2
P24_1
P24_2
AT1G36320
AT2G18220
AT4G32520
AT4G25630
AT4G26260
AT1G69200

Supplementary Figure 5. RNA-seq data demonstrates PB incuding intron retention in a group of genes. IGV visualization of six representative intron retention events detected in 6h(A) and 24h(B) treatment. Exon-intron structure of each gene was given at the bottom of each panel. The grey-color peaks indicate RNA-seq read-density across the gene. These intron retention events were marked by black arrows.

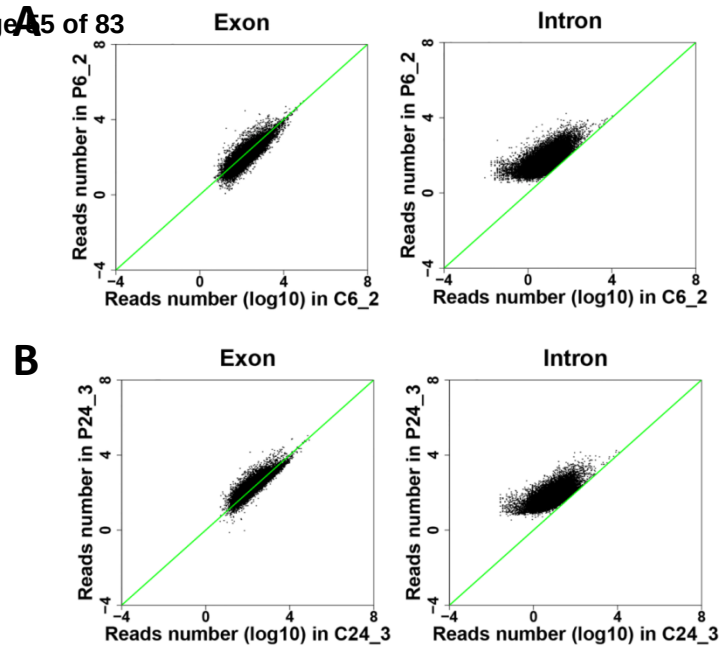

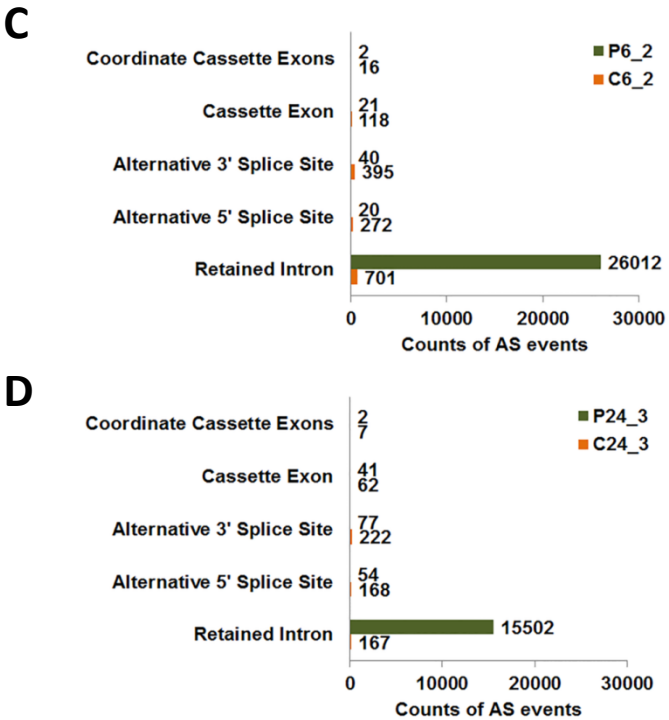

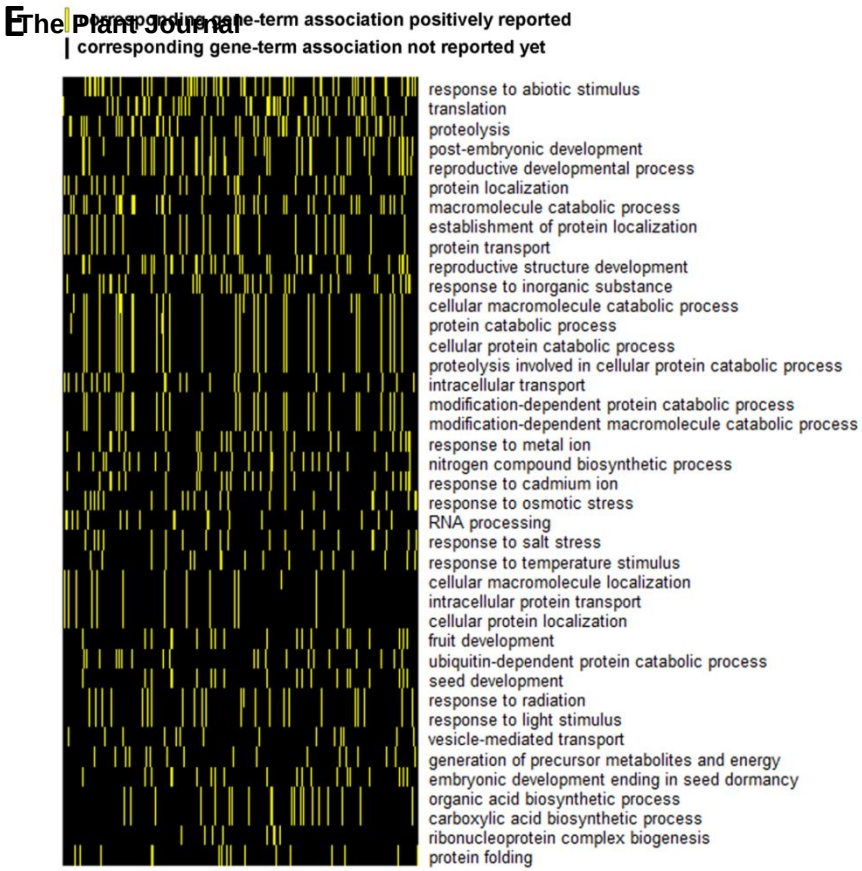

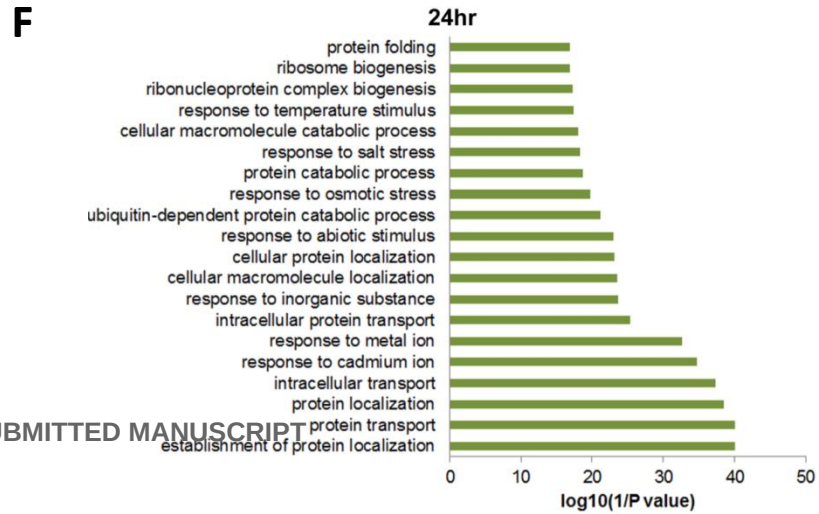

Supplementary Figure 6. Genes with intron retention in PB treatments are associated with stress responses. A and B, Comparison of intron retention between control and PB treatments. The RPKM values for the exons and introns were plotted. The expression of introns, but not exons, in PB 6h treatments showed a global up-regulation (A). The expression of introns, but not exons, in PB 6h treatments showed a global up-regulation (B). C and D, Intron retention events hugely increased in the PB-treated samples, while the other AS events (including alternative 5'SSs, 3'SSs, and exon skipping) decreased in the PB-treated 6h (C) and 24h (D) samples. E, A two-dimension representation of the relationship between the genes with perturbed splicing in PB at 24 h treatment and their corresponding functional annotation. The top 40 functional annotations were ordered according to their enrichment scores and selected for the two-dimension view indicating that the significant abnormal splicing was enriched in the response-to-abiotic-stress category. F, Functional category of genes with perturbed splicing in the 6 h treatment. Top 20 categories that were ordered by the enrichment scores were selected.

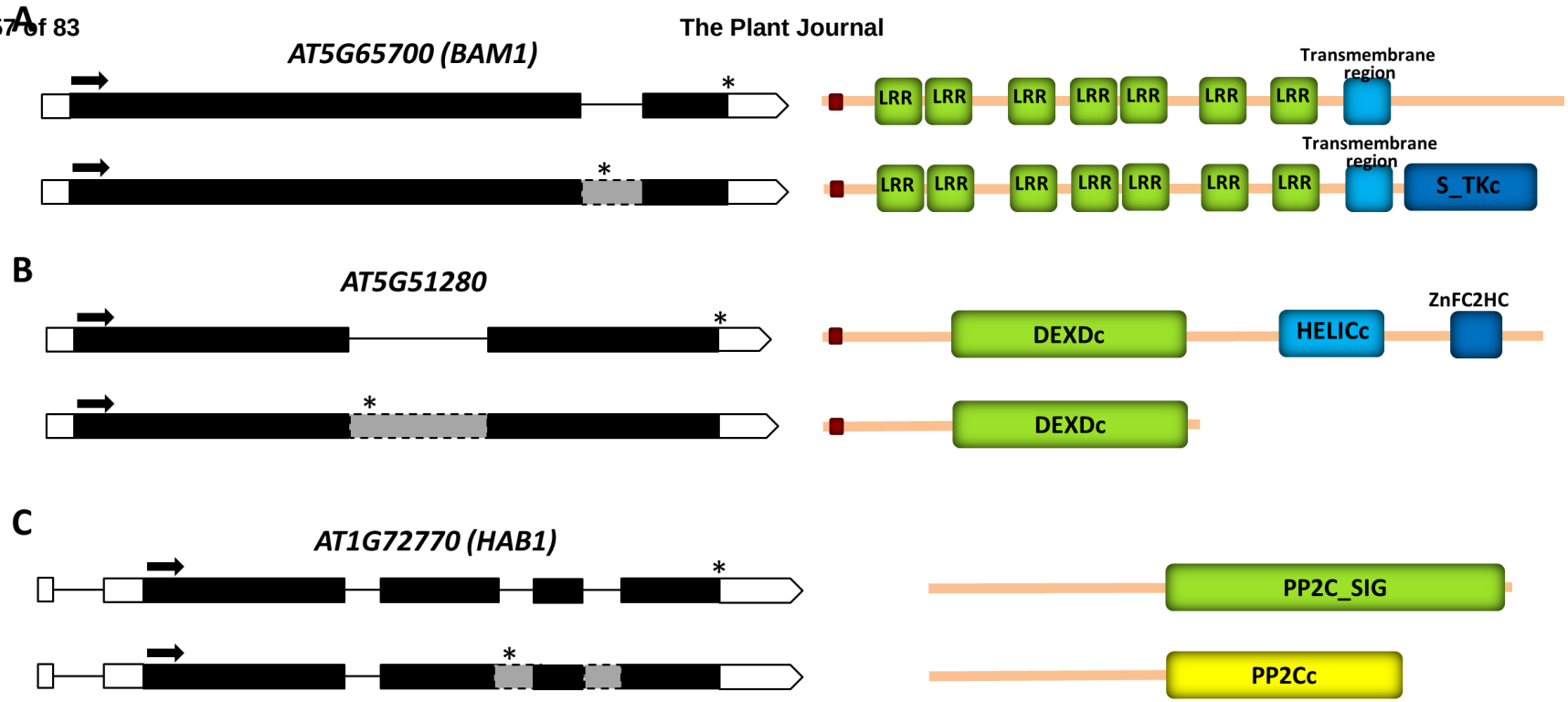
A
AT5G65700 (BAM1)
Transmembrane region
LRR
S_TKc
B
AT5G51280
ZnFC2HC
DEXDc
HELICc
C
AT1G72770 (HAB1)
PP2C_SIG
PP2Cc

Supplementary Figure 7. Comparison of proteins Encoded by known transcripts (top) and those by novel transcripts (Bottom). A, AtBAM achieved S_TKc domain (Serine/Threonine protein kinases, catalytic domain) by intron retention. B, A presumed nucleic acid binding protein containing DEXDc domain, HELICc domain, ZnFC2HC domain may produce a truncated protein containing only DEXDc domain. C, truncated PP2C protein HAB1 containing PP2Cc (Serine/threonine phosphatases, family 2C, catalytic) domain was produced. Arrows showed the position of start code, stars showed the positions of stop code. The protein domain prediction was done by online program SMART.

A

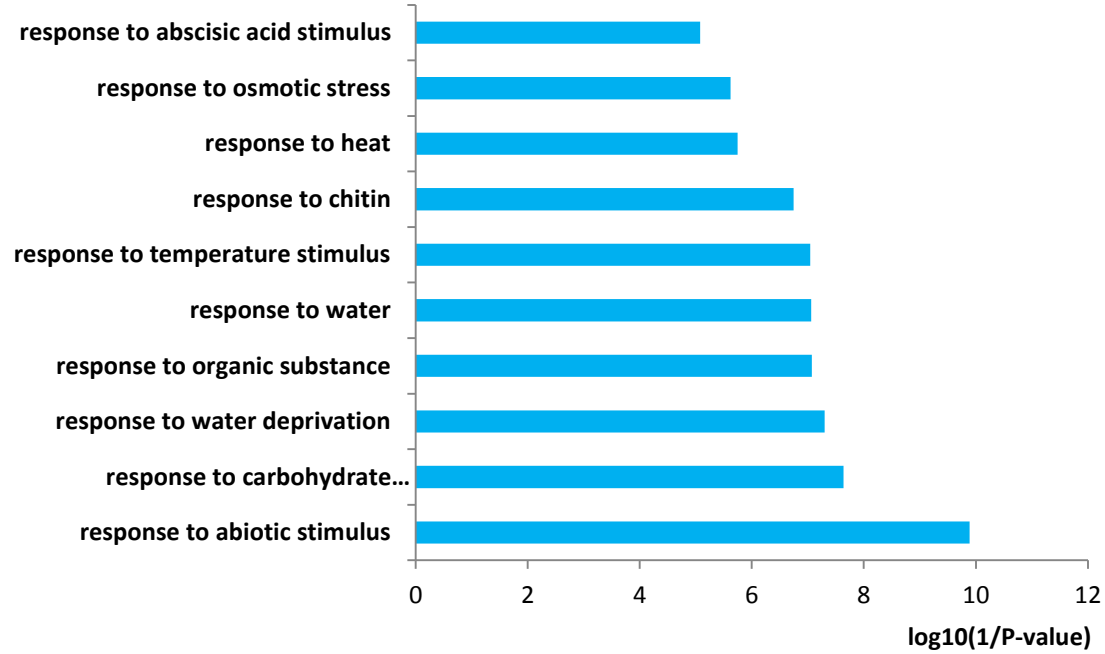

B

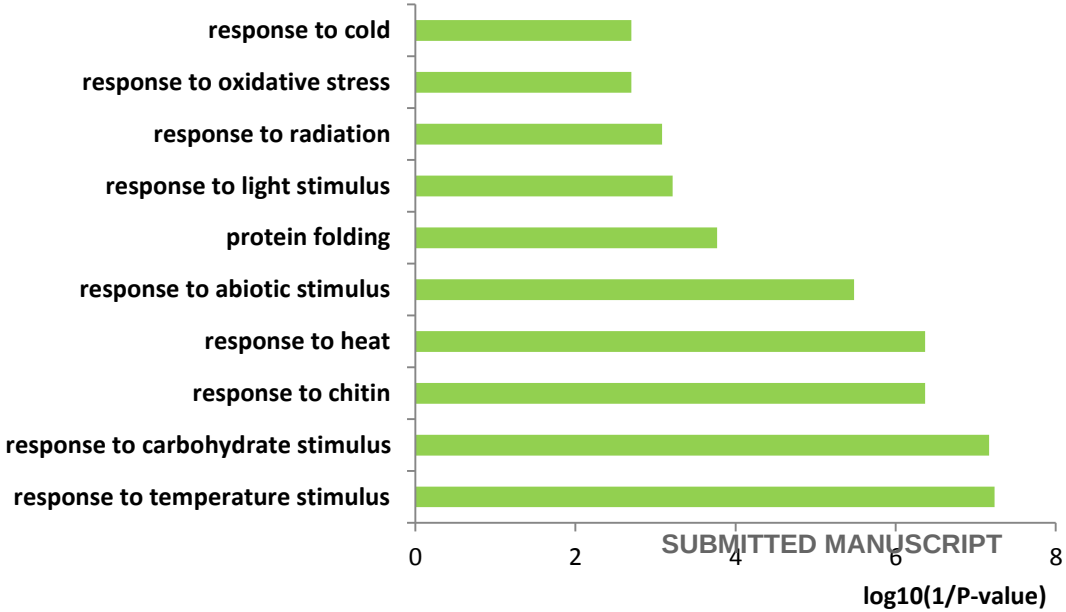

Supplementary Figure 8. Functional categorization of overlapping DE and IR genes. Functional categorization (biological process) of overlapping DE and IR genes in 6h treatment (A) and 24h treatment (B). Top 10 enriched pathways were selected to be shown.

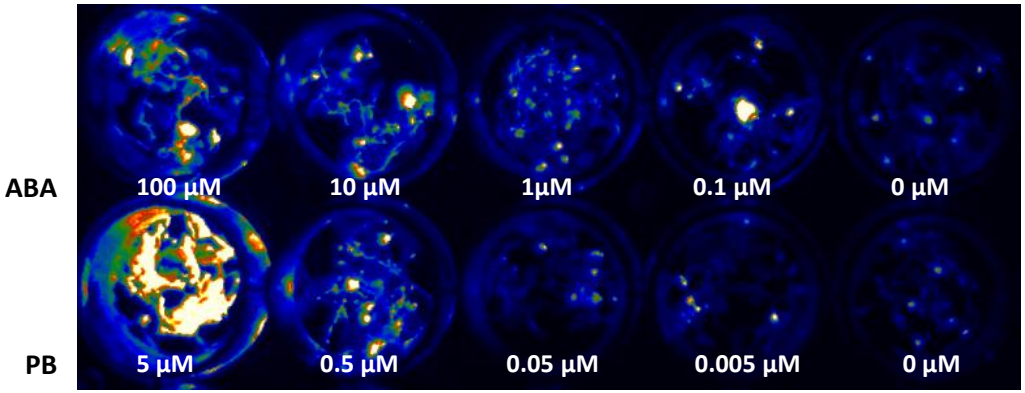
ABA
100 µM
10 µM
1µM
0.1 µM
0 µM
PB
5 µM
0.5 µM
0.05 µM
0.005 µM
0 µM

Supplementary Figure 9. Low concentration of PB induced RD29A-LUC activation in Arabidopsis seedlings. 10 days old *RD29A-LUC* transgenic seedlings were treated by different concentration of ABA and PB for 6h (the same number of plants were put in each well), then sprayed with D-luciferase and observed by CCD camera. *RD29A-LUC* was activated by low as 0.5 µM PB and 10 µM ABA, and was significantly activated by 5 µM PB, when compare with 100 µM ABA.

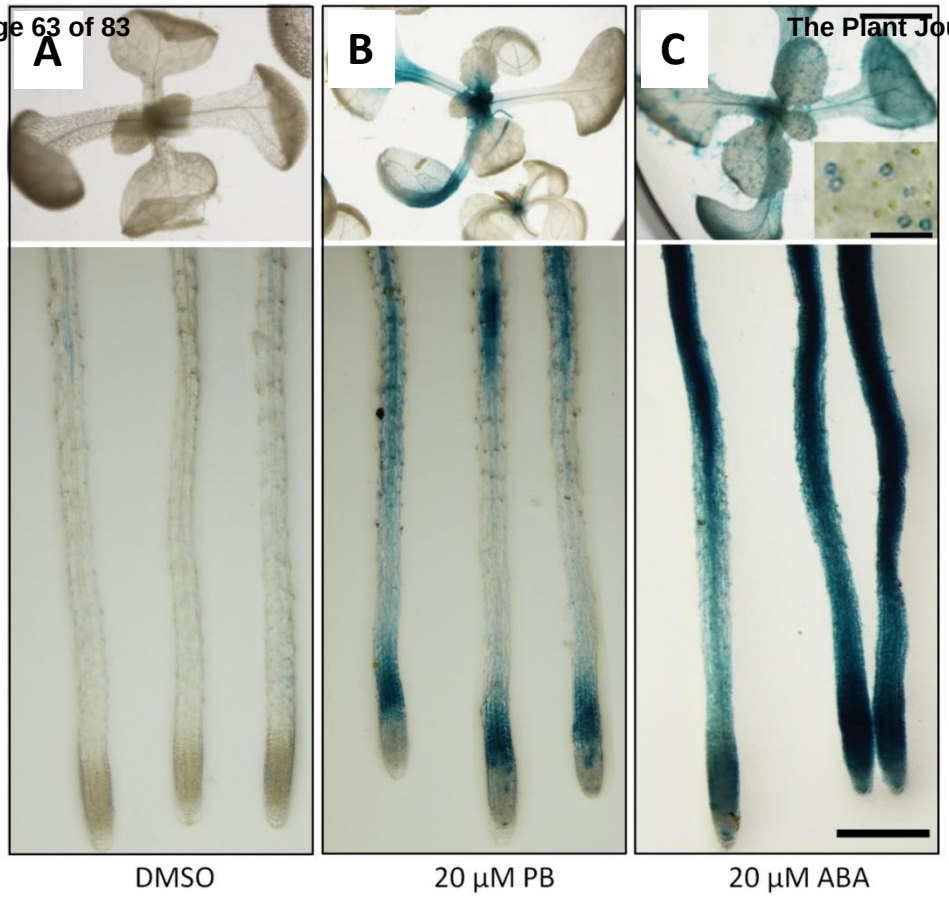
A
B
C
DMSO
20 µM PB
20 µM ABA

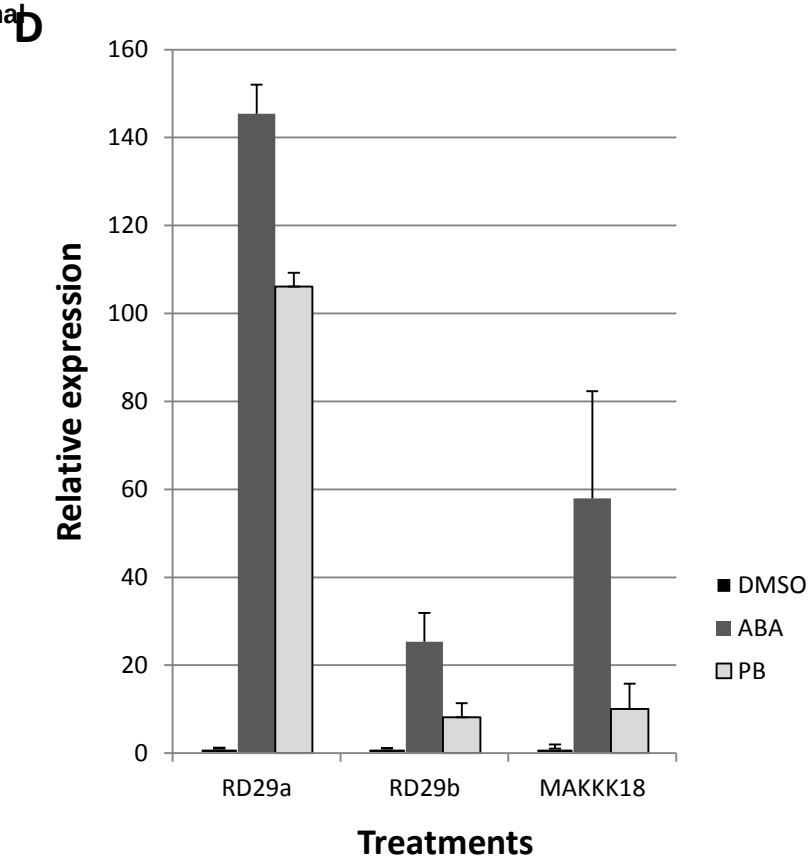
D
Relative expression
160
140
120
100
80
60
40
20
0
RD29a
RD29b
MAKKK18
Treatments
DMSO
ABA
PB

Supplementary Figure 10. PB induced RD29a, RD29b and MAKKK18 highly expression. 10 day old *MAPKKK18pro:GUS* reporter transgenic plants were incubated in 20 µM PB for 6h, followed by GUS staining. The PB treated plants (B) showed stronger GUS signal, especially in root tip and shoot tip, when compared with negative control (A), ABA was used as positive control. Scale bars, 0.5 mm(Top); 20 µm (Middle); 0.5 µm (Bottom). D, quantative RT-PCR showed PB inducing endogenous *RD29a*, *RD29b* and *MAKKK18* highly expression. The cDNAs were prepared from one week old Arabidopsis Col-0 wild type seedlings previously treated by 5 µM PB and 25 µM ABA for 6h respectively, DMSO as control.

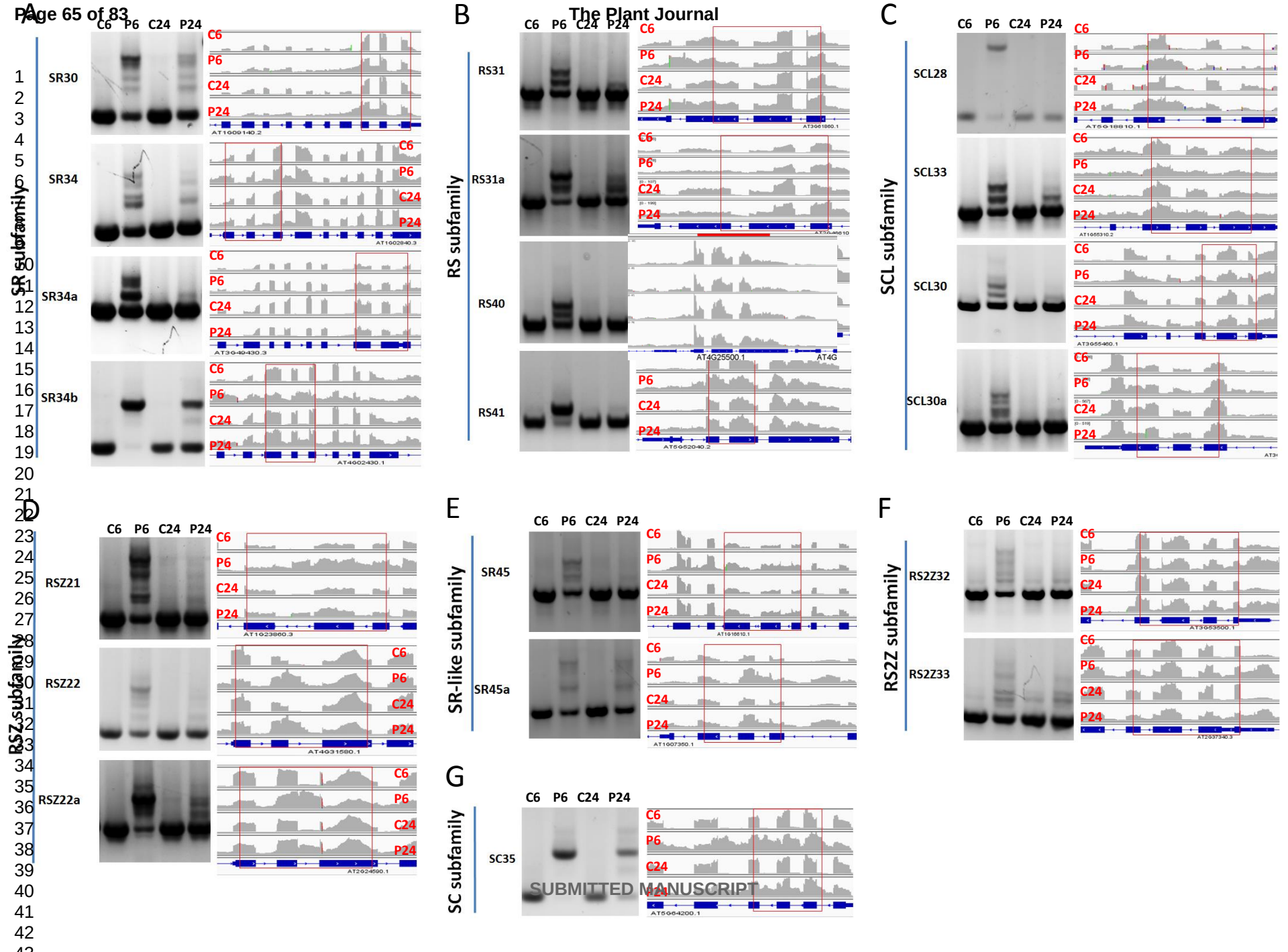

Supplementary Figure 11. PB-induced intron retention in SR and SR-like subfamily proteins.

The cDNAs were prepared from one-week-old Arabidopsis seedlings that were treated with 5 μM PB for 6 or 24 h as indicated, with DMSO as control. IGV snapshot and validation of the intron retention in SR/SR-like genes by RT-PCR using intron-flanking primers. A, SR subfamily genes, including *SR30*, *SR34*, *SR34a*, and *SR34b* underwent intron retention after PB treatments. B, RS subfamily genes, including *RS31*, *RS31a*, *RS40*, and *RS41* underwent intron retention after PB treatments. C, SCL subfamily genes, including *SCL28*, *SCL33*, *SCL30*, and *SCL30a* underwent intron retention after PB treatments. D, RSZ subfamily genes, including *RSZ21*, *RSZ22*, and *RSZ22a* underwent intron retention after PB treatments. E, SR-like subfamily genes, including *SR45* and *SR45a* underwent intron retention after PB treatments. F, RS2Z subfamily genes, including *RS2Z32* and *RS2Z33* underwent intron retention after PB treatments. G, the SC subfamily gene *SC35* underwent intron retention after PB treatments. C6, DMSO 6-h treatment; P6, PB 6-h treatment, C24, DMSO 24-h treatment, P24, PB 24-h treatment.

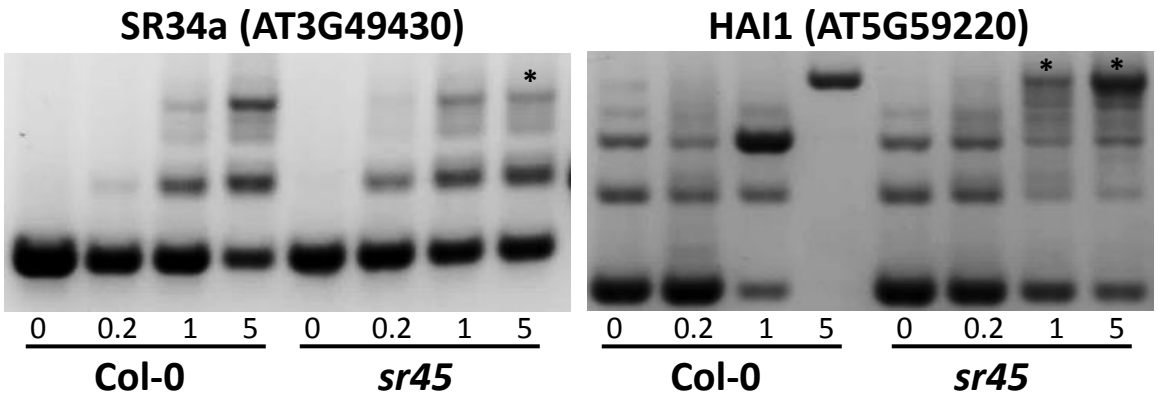
SR34a (AT3G49430)
HAI1 (AT5G59220)
*
*
*
0 0.2 1 5 0 0.2 1 5
0 0.2 1 5 0 0.2 1 5
Col-0
sr45
Col-0
sr45

Supplementary Figure 12. Comparison of intron retention intensity of genes in *sr45* and WT seedlings. cDNA were prepared from one week old Arabidopsis *sr45* and WT seedlings which were treated by 0, 0.2, 1 and 5 μM PB for6h, respectively. Intron retention of a group of gene was performed by RT-PCR using introns-flanking primers. A, SR34a (AT3G49430) , B, HAI1 (AT5G59220). The "*" represents that in our RT-PCR test, the gene contained different intron retention intensity in *sr45*, when compared with that of WT seedlings under the same treatment.

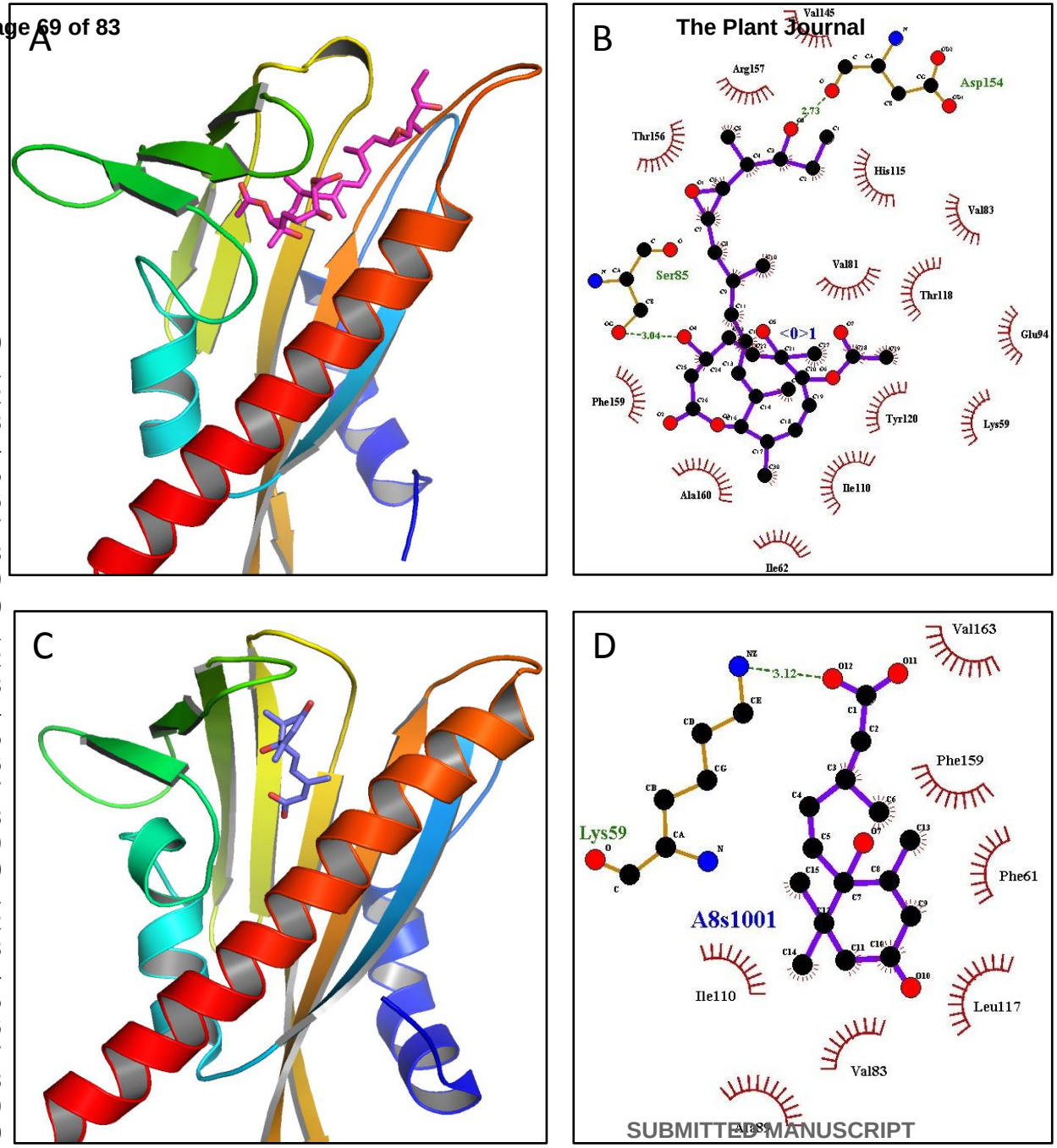

Supplementary Figure 13. *in silico* study showed PB binding to PYR/PYL proteins. A, Docking pose of top ranked binding of Pladienolide B and PYR 1 with the binding energy of -8.84 kcal/mol represented in Python Molecule Viewer 1.5.6. B, Ligand Interaction Diagram for the interacting residues. C, Docking pose of top ranked binding of Abscisic Acid (ABA) and PYR 1 Closed Conformation with the binding energy of -8.22 kcal/mol represented in Python Molecule Viewer 1.5.6. D, Ligand Interaction Diagram for the interacting residues.

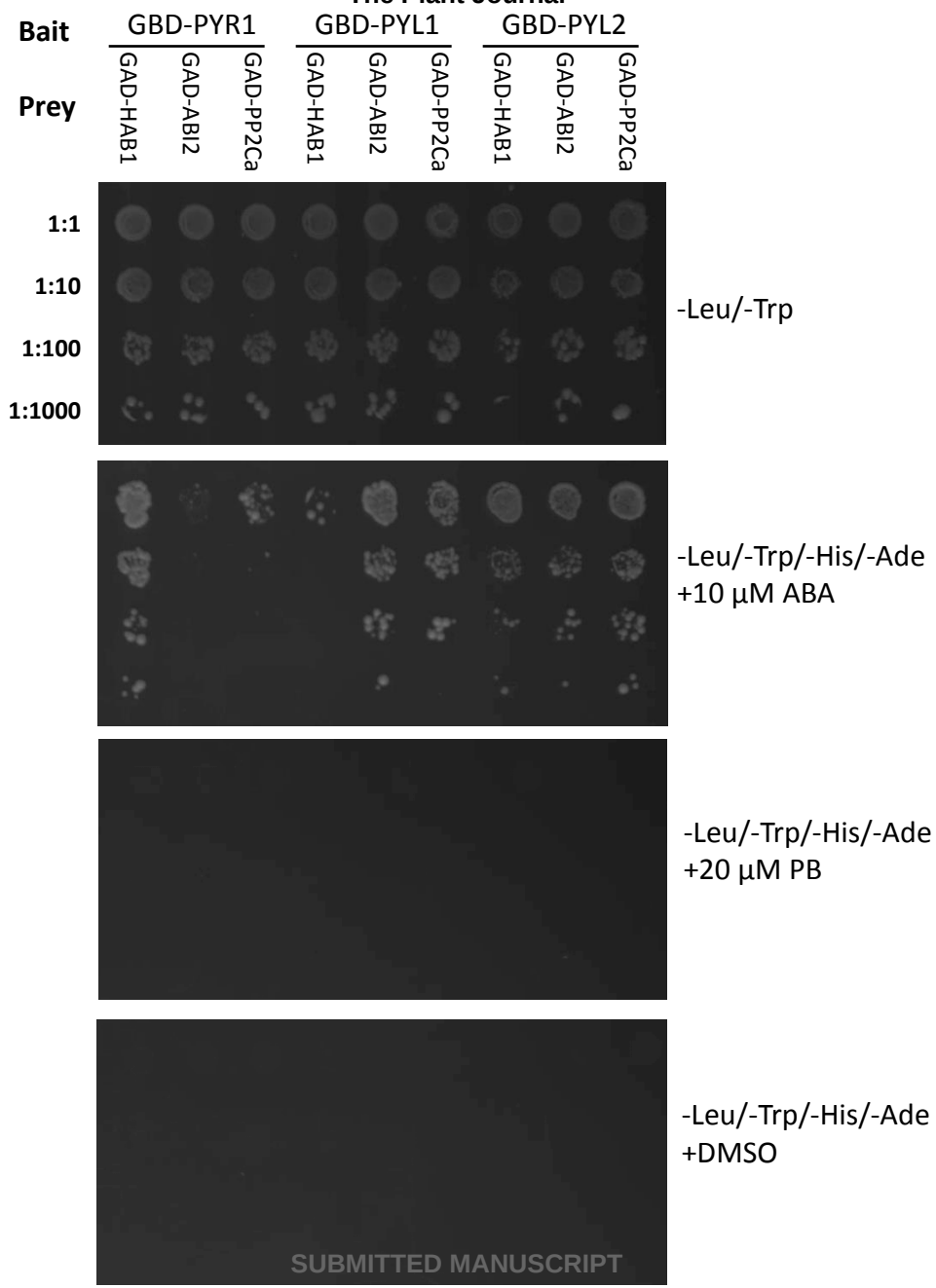

Supplementary Figure 14. Yeast two hybrid assay. PYR1, PYL1 and PYL2 fused to the GAL-DNA binding domain (GBD) were used as baits. HAB1, ABI2 and PP2Ca fused to the GAL4-activating domain (GAD) were used as preys. Dilutions (1:10, 1:100, 1:1000) of cell cultures (OD60=2) were spotted onto the plates and photographs were taken after incubation in 28 ºC for 4 days. Expressions of GBD-PYR/PYLs and GAD-PP2Cs were confirmed by growth assay on plates lacking Leu and Trp (Top panel). Induction of Interactions between PYR/PYLs and PP2Cs were tested by cell growth assay on plates lacking Leu, Trp, His and Ade (-Leu, -Trp, -His, -Ade) with addition of ABA (positive control, the second panel), DMSO (negative control, the bottom panel), and PB (the third panel).

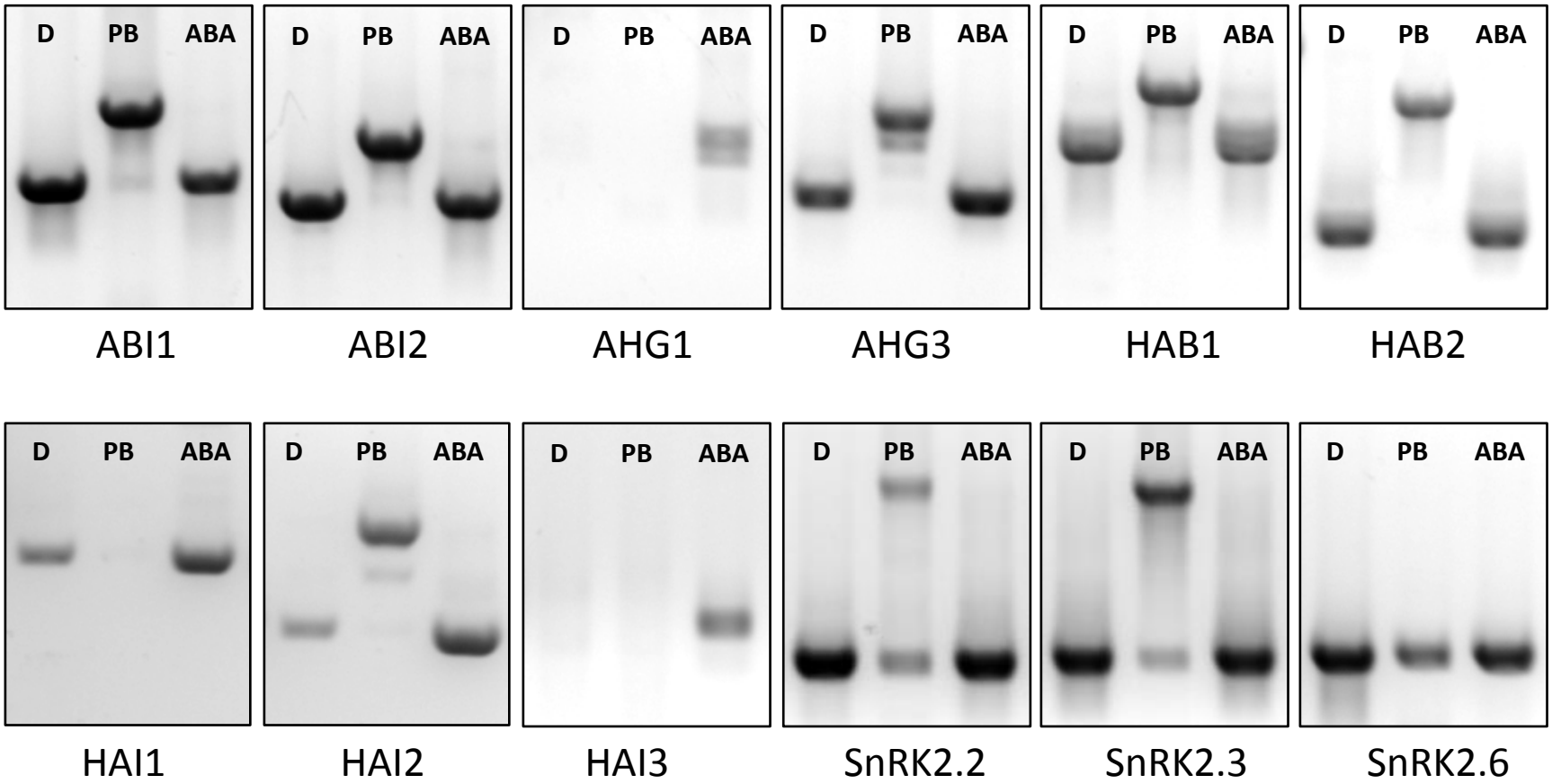
D PB ABA
ABI1
D PB ABA
ABI2
D PB ABA
AHG1
D PB ABA
AHG3
D PB ABA
HAB1
D PB ABA
HAB2
D PB ABA
HAI1
D PB ABA
HAI2
D PB ABA
HAI3
D PB ABA
SnRK2.2
D PB ABA
SnRK2.3
D PB ABA
SnRK2.6

Supplementary Figure 15. PB affected splicing of PP2C and SnRK2 genes differently. The cDNAs were prepared from one-week-old Arabidopsis seedlings that were treated with 5 µM PB or 25 µM ABA for 6 h, with DMSO as control. RT-PCR was performed using primers flanking the first exon and the last exon of each gene. ”C” for DMSO treatment, “PB” for 5 µM PB treatment and “ABA” for 25 µM ABA treatment, gene names are indicated under each panel. Nearly all functional transcripts of PP2C genes were removed by strong intron retention in PB-treated plants, whereas under the same conditions, *SnRK2.2*, *SnRK2.3*, and *SnRK2.6* kept producing functional transcripts with varying levels of intron retention. ABA induced obvious expression of some genes including: *AHG1*, *HAI1*, *HAI2*, and slightly affected the splicing pattern of *HAB1*.

A

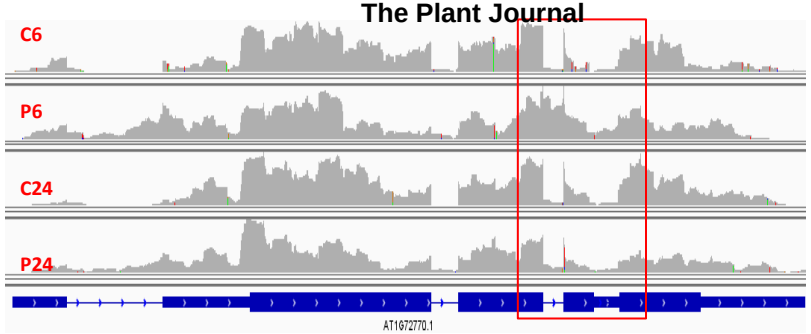
C6
P6
C24
P24
AT1G72770.1

B

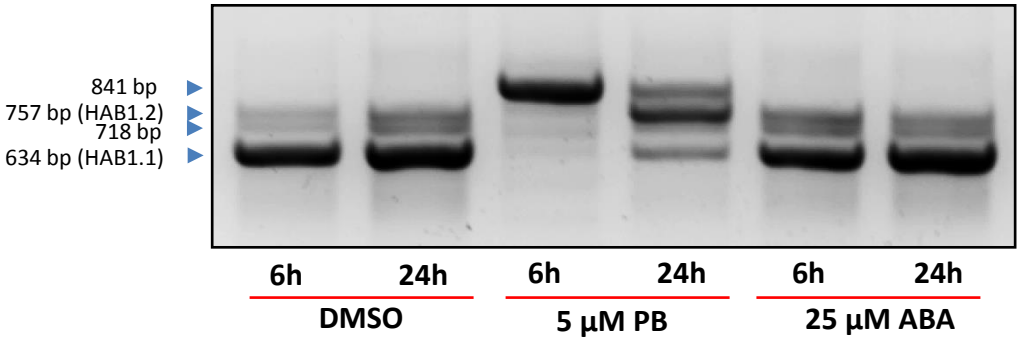
841 bp
757 bp (HAB1.2)
718 bp
634 bp (HAB1.1)
6h
24h
6h
24h
6h
24h
DMSO
5 µM PB
25 µM ABA

Supplementary Figure 16. PB treatment induced HAB1.2 isoform high expression. The cDNAs were prepared from one week old Arabidopsis seedlings which were treated by 5 µM PB and 25 µM ABA for 6/24h respectively, DMSO as control. A, snapshot of IGV for HAB1 (AT1G72770) from RNA-seq data, showing the gene structure and splicing pattern in 5 PB µM PB 6/24h treatment, DMSO as control. B, RT-PCR demonstrated that HAB1.2 variant is the major isoform after 5 PB µM PB treated for 24h. 634bp band was considered as HAB1.1 variant, and 757 bp band was HAB1.2 variant.

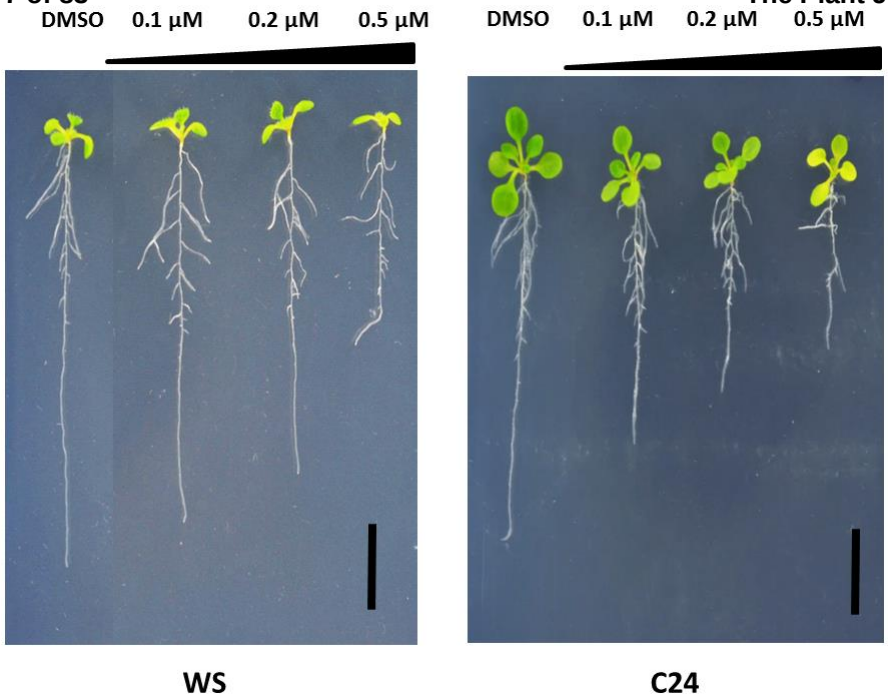

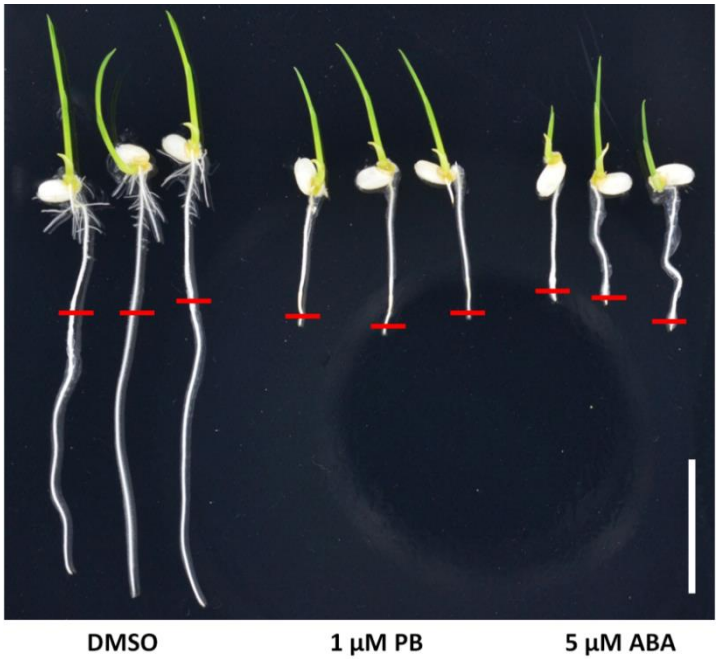

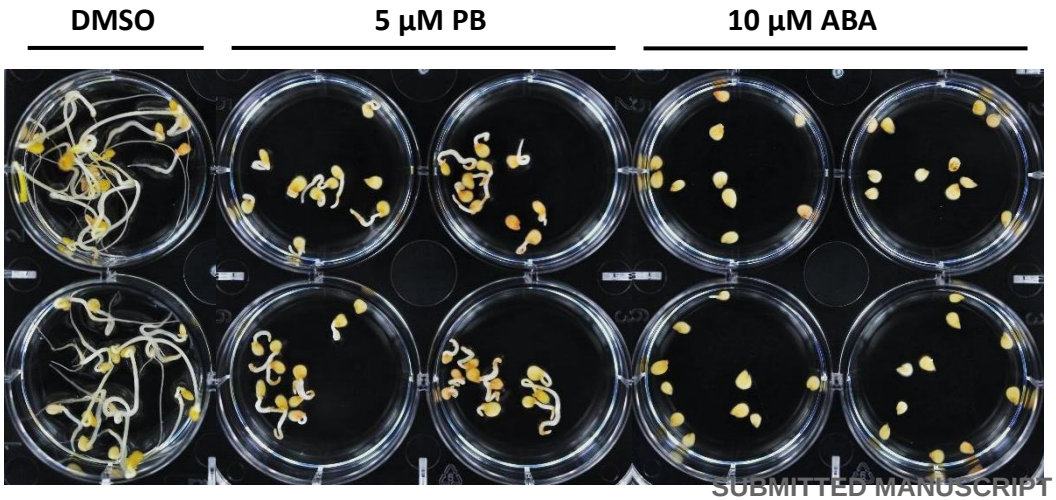

Supplementary Figure 17. Effect of PB on different ecotypes and species of plants. A, 5 day old WS-2 and C24 wild type seedlings were transferred onto ½ MS with different concentration of PB for 4 days, PB inhibited root elongation of both ecotypes, scale bar = 10 mm. B, The rice seeds were germinated on ½ MS plate for 3 days, then transfer onto ½ MS with 1 µM PB for 2 days. The red bar marks root tip of the transferring time. PB inhibits rice root elongation. Scale bar = 20mm.
C, tomato seeds was incubated in water with DMSO (negative control), 10 µM ABA (positive control), and 5 µM PB for 8 days.

Name	PDB Code	Confor-mation	Pladienolide B		Spliceostatin A		Abscisic Acid	
			ΔG	***Ki***	**ΔG**	***Ki***	**ΔG**	***Ki***
PYR1	3K3K	Open	-8.29	842.8 nM	-5.82	53.74 μM	-7.63	2.56 μM
PYR3	3KLX	Open	-7.19	5.38 μM	-6.16	30.27 μM	-6.96	6.08 μM
PYL2	3KDH	Open	-8.84	333.2 nM	-6.40	25.45 μM	-8.02	2.07 μM
PYR1	3K3K	Closed	-3.65	2.10 mM	-3.6	2.3 mM	-8.22	946.46 nM
PYL2	3KDI	Closed	-2.26	12.2 mM	-4.07	1.02 mM	-7.81	1.88 μM
PYL3	4DSC	Closed	-4.88	54.3 μM	-5.08	48.99 μM	-7.73	2.17 μM

Supplementary Table 1. Docking results with AutoDock 4.2 where **ΔG** indicates the binding energy in kcal/mol and ***Ki*** indicates the inhibition constant.

Supplementary Table 2. Informations for Primers used in this paper

Primer Name	Sequence 5'--3'	Purpose
HAB1 F1	TGAAGGAAAAATTGGTAGAGCC	isoform detection
HAB1 R1	TCAGGTTCTGGTCTTGAACTTTC	isoform detection
PYL7-F	CTGAGATCGGTTGTCTCAGAG	isoform detection
PYL7-R	CCATAGTTCCTGACCTTCCATC	isoform detection
PYL8-F	CCAGCAACTAGAAGCACTGAG	isoform detection
PYL8-R	GGTACATCAACCACAAATGACTC	isoform detection
PYL9-F	GTCAAACACATCAAAGCTCCTC	isoform detection
PYL9-R	CGATGATTTTGATACCGAGGATG	isoform detection
PYL10-F	AGGTGGAGAGCGAGTACATC	isoform detection
PYL10-R	CTTCTCTTACGCTACCAACCTC	isoform detection
ABI1-F	CGATTTGTGGAAGAAGACCTG	isoform detection
ABI1-R	GCCAAAGCCAAATGCATCCTC	isoform detection
ABI2-F1	GGACGAAGTTTCTCCTGCAG	isoform detection
ABI2-R1	CCATCTCTGGTCGTCTACCAC	isoform detection
ABI2-F2	CTTGATGGTCGAGTCACTAATGG	isoform detection
ABI2-R2	CCAACAGTTTCCGGAGCATGAG	isoform detection
AHG1-F	GGGAAGATCTCGTAAGATGGAG	isoform detection
AHG1-R	GCTTCCTTCTTCCTCCTCTTCG	isoform detection
AHG3-F	GATGGAGCTAGGGTTCTTGGAG	isoform detection
AHG3-R	GGTACAACATCCCATAGTCCATC	isoform detection
HAB1-F	ATTGAAGGAAAAATTGGTAGAGCC	isoform detection
HAB1-R	AGGTTCTGGTCTTGAACTTTCTTTG	isoform detection
HAB2-F	GATCATGAAGGGATGAGTCCAAG	isoform detection
HAB2-R	AGCTTCAAGAACCATCCTATCAG	isoform detection
HAI1-F	ACTATTGCGGCGTTTACGATG	isoform detection
HAI1-R	GTTCAACGCAACAACCTCCATG	isoform detection
HAI2-F	GCGGGAGAAGAAGAGATATGG	isoform detection
HAI2-R	CTTTCTTATCCGACAACGCTTC	isoform detection
HAI3-F	GCAAGTGTGATCTACAAACACCG	isoform detection
HAI3-R	GGACAGTCCCAATATATGACTCG	isoform detection
SnRK2.2-F	CACCGATTATGCCGATTGATTTAC	isoform detection
SnRK2.2-R	CCTAACAATATTAGGATGTCTCAATG	isoform detection
SnRK2.3-F	GGTTCTGGTAATTTCGGTGTTGC	isoform detection
SnRK2.3-R	GGATGCCTTAGTGACCTGTGG	isoform detection
SnRK2.6-F	CGAGATTGATGAGAGACAAGCAAAG	isoform detection
SnRK2.6-R	CTTTGAATCTAACGATATTGGGATG	isoform detection
ABF1-F	ACCCATAATAGTGAGGTAATAACGT	isoform detection
ABF1-R	CTTCTTACCACGGACCGGTAAG	isoform detection
ABF2-F	GGAGAAAGTTGTAGAGAGAAGGC	isoform detection
ABF2-R	GTATATTGTTTGGTCTGCCGTG	isoform detection
ABF3-F1	GTTCTGGAGAAAGTGATTGAGAG	isoform detection
ABF3-F2	GCTTATACGATGGAACTGGAAGC	isoform detection
ABF3-R	CTGATTTTTCTGCTTTTCCATGATTTC	isoform detection
ABF4.1-F	GCTTATACATTGGAACTGGAAGC	isoform detection
ABF4.2-F	gcaaagatatcttctatcccgaacc	isoform detection
ABF4-R	CTCATTCTTCTGCATTTCCACC	isoform detection

ABH1-F	GAGCAATTGGAAAACTCTTCTCC	isoform detection
ABH1-R	CCATACAAAGGAATCTTATGAGGC	isoform detection
ABI5-F	GCATGTTTTAGCTGCGCATTC	isoform detection
ABI5-R	GTAGTGGAGAGAAGACAGAGGAG	isoform detection
AHG2-F	CGTTGGGATTCTCGTACTCAG	isoform detection
AHG2-R	CTTCATGTATGCAGGTGTTGA	isoform detection
AREB3-R	GAAGACTGTAGAGAGGAGGCAG	isoform detection
AREB3-F	CTTTTGCTTCCTGAGTCTTTCG	isoform detection
CCR2-F	GATGACAGAGCTCTTGAGACTG	isoform detection
CCR2-R	CATCCTTCATGGCTTTCTCATCC	isoform detection
SAD1-F	ATGGCGAACAATCCTTCACAG	isoform detection
SAD1-R	GGTGACATCTTCAAGAACCATG	isoform detection
SR34-F	CAAATTGATTTGAAGGTTCCTCCAAG	isoform detection
SR34-R	CACGAAACTCTGATCTCCTAGATGG	isoform detection
SR45a-F	CTCCTTATGACAAGCGTCGTG	isoform detection
SR45a-R	GCCCTGCAGAACAGAGTGATC	isoform detection
SR30--F	ATGAGTAGCCGATGGAATCGTAC	isoform detection
SR30--R	GTCCATAAATTGCATCGTCTGC	isoform detection
SR45--F	CCAAGAGGACATGGTTATGTTGAG	isoform detection
SR45-R	CTTGGAGGAGATCTATATCGTCTTG	isoform detection
RSZ21-F	CGCATTCCTCGAGTTCGATGAC	isoform detection
RSZ21-R	CCTTGGAGGAGATCTTCTTCCAC	isoform detection
SCL33-F	CAATTTATGGACCCTGCTGATG	isoform detection
SCL33-R	CCTCTGACTGGAGTTAAACTGC	isoform detection
RSZ22a-F	GCGAGTTACTGAACGTGAACTC	isoform detection
RSZ22a-R	CTGTATCTAGGAGGACTGCGAC	isoform detection
RSZ33-F	GTGCGAGATGTGGATATGAAGC	isoform detection
RSZ33-R	GATCTTACAGGTGACCTGGAGTAG	isoform detection
RS31a-F	CGCGATGCTGAAGATGCAATC	isoform detection
RS31a-R	GGAGATCTCCTTCTTCGACTGC	isoform detection
SCL30a-F	CTCATATCGTCTATCCTGAGGTGAG	isoform detection
SCL30a-R	CAAGGGGGTTTGGATTCATTCAG	isoform detection
SR34a-F	GAAAGCTCCCGATCAAGAAGC	isoform detection
SR34a-R	GGAGATTTGGACGGAGACCTC	isoform detection
RSZ-F	GTACGAGATGTGGATATGAAGCG	isoform detection
RSZ-R	CTGGTGACCTGGAATAGCTTCC	isoform detection
SCL30-newF	CCGTCAGATTCTAGAAGCAGATAC	isoform detection
SCL30-newR	GACCTTGAAACTGCTCTTCCAC	isoform detection
SR31-F	CGATACACAGGACTAAGAGACCTTC	isoform detection
SR31-R	GTGTACTTTGAGGATGAACGTGATG	isoform detection
SR34b-F	GGAGGCGTTCATCACATGATG	isoform detection
SR34b-R	CTCTACCATCACGAAACACTTGAG	isoform detection
RS40-F	GACGCAGACTTCGTGTTGAATG	isoform detection
RS40-R	GACTAGCTCCTCGGCCATAATC	isoform detection
RSZ22-F	CGAGTTACTGAGCGTGAACTTG	isoform detection
RSZ22-R	CTCCTTCTGTATCTTGGAGGAGTG	isoform detection
SCL28-F	GATCACGAATCCTCTGGTCCTTC	isoform detection

SCL28-R	GCTGCATCTTCAGCATAACGATAC	isoform detection
RS41-newF1	GGAAGATGAAAGGGATGCTGAAG	isoform detection
RS41-newR	CTTCTTGTGCCTCATATTGGATG	isoform detection
SC35-F	ATGTCGCACTTCGGAAGGTC	isoform detection
SC35-R	CCTTTCCACTGCTTTGTGAGC	isoform detection
ABI1-nF	GGAGATGAGATCAACGGCTCAG	Functional transcripts detection
ABI1-nR	CCGGATCAGGAATGATGGATGG	Functional transcripts detection
ABI2-nF	GGACGAAGTTTCTCCTGCAGTC	Functional transcripts detection
ABI2-nR	CGCACTGAAGTCACTTCTGGATC	Functional transcripts detection
AHG1-nF	GGGAAGATCTCGTAAGATGGAGG	Functional transcripts detection
AHG1-nR	CCCATCGCTTGCTAATACTAAGC	Functional transcripts detection
AHG3-nR	CCGGAATCACATACGGTTTCAAG	Functional transcripts detection
AHG3-nF	CATCCTTCGTTTCTTCAACGGAAC	Functional transcripts detection
HAB1-nF	GGAGGTTGTCATTAGATTGCCAG	Functional transcripts detection
HAB2-nF	GGATCATGAAGGGATGAGTCCAAG	Functional transcripts detection
HAB2-nR	CATAAACGTCACTTCGGGATCTG	Functional transcripts detection
HAI1-nR	GTCTGCTGATTACATACGGCTTC	Functional transcripts detection
HAI1-nF	CGTCATCAGACGGAATATTCATCC	Functional transcripts detection
HAI2-nF	GACGGATCTGAGGCCGAGATAC	Functional transcripts detection
HAI2-nR	CTTGGATTCGATCCAGCTCATC	Functional transcripts detection
HAI3-nF	GTCCAAGATACGGTGTTTCTTCG	Functional transcripts detection
HAI3-nR	GACATTGCTAAGACTCCGAGAAC	Functional transcripts detection
Snrk2.2-nF	GCTGTTAAATACATCGAGAGAGGAG	Functional transcripts detection
Snrk2.2-nR	CACCTGGTAGATTCTTCAAGAACC	Functional transcripts detection
Snrk2.3-nF	GCTTGTTGCTGTCAAGTACATCG	Functional transcripts detection
Snrk2.3-nR1	GCAGGGAGATTCTTCAAGAACC	Functional transcripts detection
Snrk2.6-nF	GAACTCGTCAAGGATATTGGCTC	Functional transcripts detection
Snrk2.6-nR1	CCATATCGTCATCTATGTCCAAGC	Functional transcripts detection
RD29AqF1	AACGACGACAAAGGAAGTGG	qPCR
RD29AqR1	CATCCTTTAATCCTCCCAACC	qPCR
RD29BqF	TATGAATCCTCTGCCGTGAGAGGTG	qPCR
RD29BqR	ACACCACTGAGATAATCCGATCCT	qPCR
MAPKKK18qF	AAGCGGCGCGTGGAGAGAGA	qPCR
MAPKKK18qR	GCTGTCCATCTCTCCGTCGC	qPCR
GAPCF	TTGGTGACAACAGGTCAAGCA	qPCR
GAPCR	AAACTTGTCGCTCAATGCAAT	qPCR
AT4G35800-F	ACTCACCCACATCTCCATCTTATTC	isoform detection
AT4G35800-R	AGATCACTTTGAAACGGTCCCT	isoform detection
AT5G11670-F	GTCGAGGCCATGGCTACCAACA	isoform detection
AT5G11670-R	CCAGGCAAGTAGGTTTTGCCATC	isoform detection
AT4G35770-F	GCGAGGAAAGCAACGACAAC	isoform detection
AT4G35770-R	CGCAGCAATGTCTGTGATCG	isoform detection
AT1G55970-F	CACAACCCCACTGCCCCTGC	isoform detection
AT1G55970-R	GGTGGCTTCAGCGGCCCTTT	isoform detection
Tub-Chinu-03F	GTCAAGAGGTTCTCAGCAGTA	RT-PCR control
Tub-Chinu-03R	TCACCTTCTTGATCCGCAGTT	RT-PCR control

Materials and Methods for Supplementary Data

1. GUS staining
   6-10 days old seedlings were tested in separated experiments, GUS staining was performed in a reaction buffer of the following composition: 50 mM sodium phosphate buffer, pH 7.0, 10 mM EDTA, 0.1% Tween-20, 0.5 mM potassium ferrocyanide, 0.5 mM potassium ferricyanide, and 0.1% X-gluc. The reaction buffer with seedlings was vacuum infiltrated for 5 min and then incubated at room temperature overnight. The reaction was stopped by washing the samples with 70% ethanol, and chlorophyll pigments were bleached by incubation at 65 °C.

2. Yeast two hybrid assay
   The yeast strain Y2H Gold was uased in our experiments. The related vectors GBD-PYR/PYLs and GAD-PP2Cs were kindly sent by Dr. Pedro L.Rodriguez. After co-transformation, the transfromants successfully co-express GBD-PYR/PYLs and GAD-PP2Cs were selected by minus Trp and Leu medium. Then the positive clones were culture in minus Trp and Leu medium and followed by the protein interaction assay. For interaction assay, media lacking the four supplements (minus Trp, Leu, His and Ade) were prepared, by adding 20 μM ABA as positive control medium, and adding 0.2% DMSO as negative control, 20 μM PB was used in our experiment to test its effect on inducing PYR/PYL and PP2C interactions. At the same time, media minus Trp and Leu medium was used as control to confirm co-expression of GBD-PYR/PYLs and GAD-PP2Cs in yeast cells.

3. Docking Study
   Six crystal structures of PYR and PYL in different conformations (Supplementary Table 1) were taken from the Protein Data Bank and used to perform molecular docking with Pladienolide B and Spliceostatin A. The compounds were downloaded from the ZINC chemical database in SD format and were converted to PDB format using Open Babel 2.3.1. [1, 2].
   Flexible docking was performed using AutoDock 4.2 with specific coordinate file types for both proteins and ligands, termed PDBQT files, comprising polar hydrogen atoms, partial charges, atom types and information on the articulation of flexible molecules. The files were prepared using the AutoDock Tools 4.2 user interface [3, 4]. Water molecules were removed, polar hydrogens were added and the structures were saved as PDBQT. The flexible ligand was prepared by assigning the atom types, analyzing hydrogen bond acceptors and donors with the aromatic and aliphatic carbon atoms. The root was defined for the torsion tree from which the rotatable bonds emanate and define the flexibility of the ligand. Finally the rotatable bonds and torsion angles were assigned and the files were saved as PDBQT [5]. The grid parameters were set in accordance to the binding pocket [6]. Docking was performed using Lamarckian genetic algorithm (LGA) with population size of 150 individuals, 2.5 million energy evaluations, maximum of 27000 generations, number of top individuals to automatically survive to next generation of 1, mutation rate of 0.02, crossover rate of 0.8, 10 docking runs, and random initial positions and conformations. The probability of performing local search on an individual in the population was set to 0.06 to get optimal results [7, 8]. The complexes were then analyzed using LigPlot+ v.1.4 to generate the ligand interaction diagrams [9].

References:

1. John J.I., Teague S., Michael M., Erin S.B., Ryan G.C. ZINC: A Free Tool to Discover Chemistry for Biology. *J. Chem. Inf. Model.* **2012**, *52* (7): 1757–1768.

2. Noel M.O., Michael B., Craig A.J., Chris M., Tim V., Geoffrey R.H. Open Babel: An open chemical toolbox. *J. Cheminf.* **2011**, 3:33.

3. Cavasotto C.N., Abagyan R.A. Protein flexibility in ligand docking and virtual screening to protein kinases. *J. Mol. Biol.* **2004**; 12: 209-225.

4. Cosconati S., Forli S., Perryman A.L., Harris R., Goodsell D.S., Olson A.J. Virtual Screening with AutoDock: Theory and Practice. *Exp. Opin. Drug Disc.* **2010**; 5: 597-607.

5. Khodade P., Prabhu R., Chandra N. Parallel implementation of Autodock, J. *App. Crystal*. **2007**; 40: 598-599.

6. Goodsell D.S., Morris G.M., Olson A.J. Automated docking of flexible ligands: Applications of Autodock. *J.Mol. Recog.* **1996**; 9: 1-5.

7. Collignon B., Schulz R., Smith J.C. Task-parallel message passing interface implementation of Autodock4 for docking of very large databases of compounds using high-performance super-computers. *J. Comput. Chem*. **2011**; 32: 1202-1209.

8. Park H., Lee J., Lee S. Critical assessment of the automated AutoDock as a new docking tool for virtual screening. *Proteins.* **2006**; 65: 549-554.

9. Laskowski R.A., Swindells M.B. LigPlot+: multiple ligand-protein interaction diagrams for drug discovery. *J. Chem. Inf. Model.* **2011**; 51: 2778-2786.